

DAMTP-2007-24
hep-th/0703276

Axion-Dilaton Domain Walls and Fake Supergravity

Julian Sonner and Paul K. Townsend

Department of Applied Mathematics and Theoretical Physics
Centre for Mathematical Sciences, University of Cambridge
Wilberforce Road, Cambridge, CB3 0WA, UK

Abstract

Dynamical systems methods are used to investigate domain-wall solutions of a two-parameter family of models in which gravity is coupled to an axion, and to a dilaton with an exponential potential of either sign. A complete global analysis is presented for (i) constant axion and (ii) flat walls, including a study of bifurcations, and a new exact domain-wall solution with non-constant axion. We reconsider ‘fake supergravity’ issues in light of these results. We show, by example, how domain walls determine multi-valued superpotentials that branch at stationary points that are not stationary points of the potential, and we apply this result to potentials with anti-de Sitter vacua. We also show by example that ‘adapted’ truncation to a single-scalar model is sometimes inconsistent, and we propose a ‘generalized’ fake supergravity formalism that applies in some such cases.

Contents

1	Introduction	1
1.1	Preliminaries	5
2	Constant axion	6
2.1	Global structure	7
2.2	Fixed points	9
2.2.1	$\Lambda < 0$	10
2.2.2	$\Lambda > 0$	11
2.3	Bifurcations at infinity	11
2.4	Trajectories vs solutions	15
3	Flat walls	16
3.1	Global Structure and Fixed Points	17
3.1.1	Boundary fixed points	18
3.1.2	Interior fixed points	18
3.2	Bifurcations	19
3.3	An exact axion-dilaton domain-wall solution	21
4	Supersymmetry	25
4.1	Single-scalar models revisited	26
4.1.1	Branched superpotentials	27
4.1.2	Asymptotically adS walls	28
4.2	E Pluribus Unum?	31
4.3	Axion-dilaton fake supergravity	33
5	Discussion	36

1 Introduction

In a recent paper [1] we addressed the problem of domain wall solutions of the coupled Einstein-dilaton equations, in d spacetime dimensions, using dynamical systems methods imported from studies of cosmological solutions of the same model [2, 3]. We recovered efficiently and simply many of the previously known exact results on dilaton domain walls and found some new ones. In addition, we obtained a qualitative overview of the entire space of domain wall solutions in this model. For example, the “Janus” walls that were studied in [4] were shown to have a natural interpretation as marginal bound states of a new type of dilaton domain wall that we called a “separatrix-wall”. This result is reminiscent of BPS solitons and it suggested a ‘hidden’ supersymmetry of the separatrix-wall that has since been confirmed [5].

One purpose of this paper is to continue our dynamical systems investigations of domain walls in a more general class of models for which both the dilaton field σ

and a pseudo-scalar ‘axion’ field χ are coupled to a d -dimensional metric g via the Lagrangian density

$$\mathcal{L} = \sqrt{-\det g} \left[R - \frac{1}{2} (\partial\sigma)^2 - \frac{1}{2} e^{\mu\sigma} (\partial\chi)^2 - V \right], \quad (1.1)$$

where μ is an axion-dilaton coupling constant, and the potential function V takes the form

$$V = \Lambda e^{-\lambda\sigma}, \quad (1.2)$$

where λ is the dilaton ‘coupling constant’, and Λ a non-zero ‘cosmological’ constant. This is the unique form of the potential that preserves an invariance of the equations of motion under the ‘dilation’ $g \rightarrow e^\omega g$, for constant parameter ω , by virtue of the inhomogeneous transformation $\sigma + \omega/\lambda$ of the dilaton field. Only the sign of Λ is relevant when $\lambda \neq 0$, as a shift of σ is then equivalent to a scaling of Λ . We may assume that $\lambda \geq 0$ without loss of generality, as in [1], but then μ could have either sign; its absolute value is related to the radius of curvature of the hyperbolic target space for which (σ, χ) are coordinates. The $\mu = 0$ case, which corresponds to a flat target space, has been investigated (in a cosmology context) in [6, 7].

We have recently studied cosmological solutions for this class of axion-dilaton model [8], following the work of [9] on a particular model for which flat universes were shown to expand and contract quasi-periodically in a certain non-Einstein frame. We found a range of the parameters (λ, μ) , for which generic flat universes are eternally expanding, in Einstein frame, but undergo a medium-time and/or late-time oscillation between acceleration and deceleration. These results were one motivation for the present work because if one allows for both signs of the potential then the family of dynamical systems governing cosmological solutions is the same as the family of dynamical systems governing domain-wall solutions (illustrating the general ‘Domain-Wall/Cosmology Correspondence’ [5]), and the quasi-cyclic nature of many trajectories could imply novel behaviour for associated holographic renormalization group flows.

The equations for either domain walls or cosmologies in a model with n scalar fields define an autonomous dynamical system of dimension $2n + 1$, once account is taken of the reparametrization constraint. Reparametrization invariance implies that the physical phase space is actually only $2n$ -dimensional but the dynamics on this space is not necessarily autonomous. Thus, even for $n = 1$ we should expect to have to consider a 3-dimensional system, and a 5-dimensional system for $n = 2$. However, a reduction to an autonomous 2-dimensional system is possible for $n = 1$ when the potential is an exponential, as is well-known; this case arises in the present context from the restriction to constant axion. Less well-known is the fact that the 5-dimensional dynamical system for $n = 2$ models of the above axion-dilaton type has a 2-dimensional autonomous subsystem when the restriction is made to flat domain walls, or cosmologies, and the behaviour is essentially determined by this subsystem.

Here we present a detailed study of the 2-dimensional dynamical systems corresponding to (i) constant axion and (ii) flat domain walls, for either sign of Λ and as a function of the two parameters (λ, μ) . Dynamical systems methods are particularly

powerful in these cases because trajectories are easily visualized, and chaotic dynamics is excluded. Case (i) has been investigated previously in [2, 3, 7] (in the context of cosmology) and in our previous paper [1] (in the context of domain walls) but here we present a complete global analysis. In particular, we show that the global phase space, allowing for both signs of Λ , is a sphere. We also extend the analysis of bifurcations to those that occur ‘at infinity’, which corresponds to a great circle on the sphere separating the trajectories with $\Lambda > 0$ from those with $\Lambda < 0$. Case (ii) has been investigated previously in the context of cosmology [8, 9] for one sign of Λ . Here we present a complete global analysis that includes both signs of Λ . One new result is an exact flat domain-wall solution with non-constant axion field. It corresponds to a fixed point of the dynamical system and for $\Lambda < 0$ it is the domain-wall analog of the $\Lambda > 0$ axion-dilaton cosmological solution found in [8].

For some values of the parameters (λ, μ) and a choice of the sign of Λ , the model defined by (1.1) may be a truncation of a supergravity theory. For example, the Freedman-Schwarz $N = 4$, $d = 4$, supergravity [10] has $2\lambda = -\mu = 2$, and¹ $\Lambda < 0$, and in this context one may ask whether any given domain wall solution preserves some fraction of the supersymmetry. A necessary condition for partial preservation of supersymmetry is that the domain wall solution admit a Killing spinor, which is a spinor field satisfying the equation that results from the requirement of vanishing supersymmetry variation of the gravitino field(s); this equation depends not only on the spacetime metric but also on the (pseudo)scalar fields through a ‘superpotential’, which determines the scalar potential. More generally, one can extend the notion of a ‘supersymmetric’ domain wall solution beyond the supergravity context by allowing the superpotential to be any function that yields the potential according to a d -dimensional generalization of the formula that applies in the supergravity case [11]. Domain wall solutions admitting Killing spinors with respect to such a superpotential [12, 13] are then said to be ‘fake supersymmetric’ solutions of a ‘fake supergravity’ [4]. The relevance of this idea is that ‘fake’ supersymmetry suffices for classical stability.

Another purpose of this paper is to use the axion-dilaton models as a ‘laboratory’ for further investigations of fake supersymmetry, but we will also have more to say about the simpler Einstein-dilaton model of [1]. It was shown in [4, 1] that ‘almost all’ flat domain-wall solutions of any single-scalar model are fake supersymmetric because the solution can be used to construct a superpotential with respect to which the first-order Killing-spinor integrability equations are satisfied. This result was extended to particular curved domain walls in [13] and to ‘almost’ all curved domain walls in [5]. The qualification ‘almost’ arises from a monotonicity condition. Typically, this condition is violated at isolated points (although non-isolated accumulation points occur in walls that are asymptotic to perturbatively unstable anti-de Sitter vacua [14]). In this case the associated superpotential is multi-valued and the domain wall is ‘piecewise’ supersymmetric with respect to it [5]. We illustrate this phenomenon here with a simple double-valued superpotential that can be found from an exact flat domain wall solution of [1]. This example illustrates another significant feature, intrinsic to the phenomenon: the branch point of the superpotential is a stationary

¹This model was incorrectly identified in [8] as one with $\Lambda > 0$.

point that is not a stationary point of the potential. We use the insights gained from this example to discuss general potentials with adS vacua, showing that there again exist conditions under which some superpotential will be double-valued and hence not defined for all values of the scalar field, as was recently argued for a particular potential [15].

Fake supergravity models with multiple scalar fields were investigated briefly in [13] and more extensively in [16], where it was observed that for any given domain-wall solution there exist, at least locally, ‘adapted’ target space coordinates such that all scalar fields but one are constant [16]. The given solution is thus manifestly a solution of the single-scalar model obtained by the obvious truncation in the new variables. It is also (if it satisfies the monotonicity condition) a supersymmetric solution of the ‘adapted’ single-scalar model [5]. Thus, results on fake supersymmetry for single-scalar models can be extended simply to multi-scalar models. However, there is a difficulty with this extension (in addition to possible global problems arising from the local nature of the ‘adapted’ target space coordinates). To address stability of a given solution one needs to consider solutions ‘nearby’ the given one. It may happen, if the single-scalar truncation is inconsistent, that there are no nearby solutions of the single-scalar model that are also solutions of the multi-scalar model, in which case the fake supersymmetry of the domain wall as a solution of the single-scalar model is irrelevant to its stability. The *consistency* of the single-scalar truncation is therefore important. Consistency is manifest for the restricted class of multi-scalar models considered in [13] and probable (to the extent that we have understood the issue) for the more general models of [16]. For a solution that is not known explicitly, we know of no way to determine whether the associated adapted truncation is consistent. This is where the axion-dilaton models of this paper become useful. The new domain-wall solution with non-constant axion mentioned earlier provides a simple example of an intrinsically multi-scalar domain-wall solution for which adapted target space coordinates can be found explicitly; this is possible because the solution is explicit. It turns out that the associated single-scalar truncation is inconsistent, except in a limit in which the solution degenerates to one in which the axion field is constant. This shows that consistency of adapted truncations is not automatic, and this limits the utility of this particular multi-scalar extension of the notion of fake supersymmetry.

This result motivates an extension of the notion of fake supergravity to models involving at least two (pseudo)scalar fields. We propose such an extension, modeled on the coupling of $d = 4$ supergravity to a complex chiral superfield, and we find that a one-parameter subfamily of our two-parameter family of axion-dilaton models can be regarded as ‘fake supergravities’ in this extended sense. Fortunately, existence of the exact fixed-point domain-wall solution is compatible with this restriction of the parameters when $\Lambda < 0$, and we are able to address the issue of fake supersymmetry in an *untruncated* context in this case. Our conclusion will be that the axion-dilaton domain wall solution for which the adapted single-scalar truncation is inconsistent is *not* fake supersymmetric.

1.1 Preliminaries

As in [1], we introduce the d -dependent constants

$$\alpha = \sqrt{\frac{d-1}{2(d-2)}}, \quad \beta = 1/\sqrt{2(d-1)(d-2)}. \quad (1.3)$$

and express the spacetime metric in terms of a function $\varphi(z)$ through the domain-wall ansatz

$$ds^2 = e^{2\alpha\varphi} f^2 dz^2 + e^{2\beta\varphi} d\Sigma_k^2, \quad (1.4)$$

where $f(z)$ is an additional arbitrary function that allows us to maintain invariance under z -reparametrizations, and $d\Sigma_k^2$ is the metric of a $(d-1)$ -dimensional maximally symmetric spacetime with inverse radius of curvature k ; i.e. such that the scalar curvature is $k(d-1)(d-2)$. We may restrict k to take the values $-1, 0, 1$, and we then have a domain wall spacetime that is foliated by anti-de Sitter (adS), Minkowski or de Sitter (dS) spacetimes, respectively. Invariance of the solution under the isometries of the metric implies that the fields (σ, χ) can depend only on z . The field equations now reduce to equations of motion, and a constraint, for the variables (φ, σ, χ) that are the Euler-Lagrange equations of the effective Lagrangian²

$$L_{eff} = \frac{1}{2} [f^{-1} (\dot{\varphi}^2 - \dot{\sigma}^2 - e^{\mu\sigma} \dot{\chi}^2) + f e^{2\alpha\varphi} (k\beta^{-2} e^{-2\beta\varphi} - 2\Lambda e^{-\lambda\sigma})]. \quad (1.5)$$

The equations of motion for the gauge choice

$$f = e^{-\alpha\varphi + \frac{1}{2}\lambda\sigma} \quad (1.6)$$

are equivalent to the equations

$$\begin{aligned} \ddot{\varphi} &= -\alpha\dot{\varphi}^2 + \frac{1}{2}\lambda\dot{\varphi}\dot{\sigma} - 2\alpha\Lambda + \frac{k}{2\alpha\beta^2} e^{\lambda\sigma - 2\beta\varphi}, \\ \ddot{\sigma} &= -\alpha\dot{\sigma}\dot{\varphi} + \frac{1}{2}(\lambda - \mu)\dot{\sigma}^2 + \frac{1}{2}\mu\dot{\varphi}^2 + (\mu - \lambda)\Lambda \end{aligned} \quad (1.7)$$

and the constraint

$$\dot{\chi}^2 = e^{-\mu\sigma} \left[\dot{\varphi}^2 - \dot{\sigma}^2 + 2\Lambda - \frac{k}{\beta^2} e^{\lambda\sigma - 2\beta\varphi} \right]. \quad (1.8)$$

The χ equation of motion follows from differentiation of the constraint.

For the two special cases (i) $\dot{\chi} = 0$ and (ii) $k = 0$, the above equations contain a 2-dimensional autonomous dynamical system for the variables

$$u = \dot{\sigma}, \quad v = \dot{\varphi}. \quad (1.9)$$

²Because of the inclusion of the function f in the ansatz, this effective Lagrangian can also be obtained by substitution of the ansatz in the Lagrangian density (1.1), whereas this is true only for $k = 0$ for an ansatz that fixes the z -reparametrization invariance.

We shall consider $\Lambda < 0$ and $\Lambda > 0$ in turn. For both cases, it is convenient to define

$$\lambda_c = 2\sqrt{\alpha\beta} = \sqrt{\frac{2}{d-2}}, \quad \lambda_h = 2\alpha = \sqrt{d-1} \lambda_c. \quad (1.10)$$

These quantities have a general convention-independent significance, but take the above particular values in our conventions.

Finally, although the gauge choice (1.6) is convenient for our particular models, it has the disadvantage that z is not (generically) an affine parameter when $\lambda \neq 0$. It is related to an affine distance parameter \tilde{z} through the differential equation

$$d\tilde{z} = e^{\frac{1}{2}\lambda\sigma(z)} dz, \quad (1.11)$$

and the spacetime metric takes a standard form in terms of \tilde{z} ; for flat walls we have

$$ds^2 = e^{\lambda\sigma} d\tilde{z}^2 + e^{2\beta\varphi} ds^2(\mathbb{E}^{(1,d-2)}), \quad (1.12)$$

where (perpetrating a slight abuse of notation to avoid the introduction of new symbols for dependent variables) φ is now to be understood as that function of \tilde{z} obtained by use of the inverse function $z(\tilde{z})$ in $\varphi(z)$, and similarly for σ .

2 Constant axion

For $\dot{\chi} = 0$, the equations (1.7) and constraint (1.8) yield the autonomous dynamical system

$$\begin{aligned} \dot{u} &= -\alpha uv + \frac{1}{2}\lambda u^2 - \lambda\Lambda \\ \dot{v} &= -\beta v^2 - \frac{1}{2\alpha}u^2 + \frac{1}{2}\lambda uv - 2\beta\Lambda \end{aligned} \quad (2.1)$$

and the constraint

$$v^2 - u^2 + 2\Lambda = \frac{k}{\beta^2} e^{\lambda\sigma - 2\beta\varphi}. \quad (2.2)$$

The constraint shows that the $k = -1$ trajectories are separated from the $k = 1$ trajectories by the $k = 0$ hyperbola $v^2 - u^2 + 2\Lambda = 0$. As only the sign of Λ is relevant for $\lambda > 0$, we effectively have two two-parameter families of dynamical systems, one for $\Lambda > 0$ and another for $\Lambda < 0$. In the absence of limit cycles, the phase-plane portraits of these two systems are determined by the fixed points. Poincaré index considerations show that limit cycles cannot arise for $\Lambda > 0$, nor for $k \leq 0$ [1]. This observation leaves open the possibility of $k = 1$ limit cycles in the $\Lambda < 0$ system, but in this case the constraint (2.2) implies that $v^2 > 0$, and hence that $\varphi(z)$ is a ‘monotone function’, which is incompatible with the existence of a limit cycle.

We now present an analysis of the global structure of the $\Lambda > 0$ and $\Lambda < 0$ dynamical systems. As we shall show, individually the global phase space for each system is a disc, but the two discs can be viewed as two hemispheres of a topological sphere³

³This result was stated without proof in [8], where phase planes for the two hemispheres were

2.1 Global structure

Define new phase-plane coordinates (x_+, y_+) by

$$(x_+, y_+) = \frac{1}{\sqrt{u^2 + v^2 + 2\Lambda}} (u, v), \quad (u, v) = \sqrt{\frac{2\Lambda}{1 - x_+^2 - y_+^2}} (x_+, y_+). \quad (2.3)$$

This maps the $k = 0$ hyperbola $u^2 - v^2 = 2\Lambda$ into the lines $2x_+^2 = 1$. For $\Lambda > 0$ the entire (u, v) plane is mapped to the interior of the unit circle in the (x_+, y_+) plane. For $\Lambda < 0$ the domain of the map is the exterior of the circle of radius $\sqrt{2|\Lambda|}$ in the (u, v) plane, which is mapped to the exterior of the unit circle in the (x, y) plane. Thus, the new coordinates yield a description of the dynamical system that includes both signs of Λ , with Λ effectively changing sign on the unit circle; this is possible because the value of Λ becomes irrelevant as the unit circle is approached.

The equations for the dynamical system in the (x_+, y_+) coordinates are

$$\begin{aligned} \frac{dx_+}{dz_+} &= \frac{1}{\lambda_h} x_+ y_+ (x_+^2 - y_+^2) + (x_+^2 + y_+^2 - 1) \left[\frac{1}{2} \lambda - \lambda x_+^2 + \frac{1}{\lambda_h} x_+ y_+ \right] \\ \frac{dy_+}{dz_+} &= -\frac{1}{\lambda_h} x_+^2 (x_+^2 - y_+^2) + (x_+^2 + y_+^2 - 1) \left[\beta - \lambda x_+ y_+ + \frac{1}{\lambda_h} x_+^2 \right], \end{aligned} \quad (2.4)$$

where z_+ is a new independent variable such that

$$\dot{z}_+ = \sqrt{\frac{2\Lambda}{1 - x_+^2 - y_+^2}}. \quad (2.5)$$

Observe that the unit circle in the (x_+, y_+) plane is a fixed set of the system defined by the equations (2.4). Defining polar coordinates (r, θ) by $x_+ = r \cos \theta$ and $y_+ = r \sin \theta$, we find that

$$r'|_{r=1} = 0, \quad \theta'|_{r=1} = -\frac{1}{\lambda_h} \cos \theta \cos 2\theta. \quad (2.6)$$

This determines the flows on the unit circle, on which there are six fixed points, two at the angles for which $\cos \theta = 0$ and four at the angles for which $\cos 2\theta = 0$. The trajectories for $r < 1$ are those of the original dynamical system restricted to $\Lambda > 0$. Similarly, the trajectories for $r > 1$ are those of the original dynamical system restricted to $\Lambda < 0$, but the description of this system in the (x_+, y_+) coordinates is incomplete because the region in the (u, v) plane with $u^2 + v^2 \leq 2|\Lambda|$ is not covered when $\Lambda < 0$.

We may remedy the incompleteness of the (x_+, y_+) coordinates for $\Lambda < 0$ by defining a different set of new coordinates (x_-, y_-) , by

$$(x_-, y_-) = \frac{1}{\sqrt{u^2 + v^2 - 2\Lambda}} (u, v), \quad (u, v) = \sqrt{\frac{2\Lambda}{x_-^2 + y_-^2 - 1}} (x_-, y_-). \quad (2.7)$$

sketched for some cases of relevance to cosmic acceleration. Only $\Lambda > 0$ cosmologies were considered in [8], since cosmic acceleration is possible only in this case, but it should be remembered that this corresponds to $\Lambda < 0$ in the domain wall context, and that the sign of k is different.

This maps the $k = 0$ hyperbola $u^2 - v^2 = 2\Lambda$ into the lines $2y_-^2 = 1$. The domain of this map for $\Lambda < 0$ is the *entire* (u, v) plane, which is now mapped to the *interior* of the unit circle in the (x_-, y_-) plane. It is now for $\Lambda > 0$ that the domain is the region in the (u, v) plane exterior to the circle of radius $\sqrt{2\Lambda}$, and this region is mapped to the exterior of the unit circle in the (x_-, y_-) plane. The equations for the dynamical system in the (x_-, y_-) coordinates are

$$\begin{aligned}\frac{dx_-}{dz_-} &= \frac{1}{\lambda_h} x_- y_- (x_-^2 - y_-^2) + (x_-^2 + y_-^2 - 1) \left[-\frac{1}{2} \lambda + \left(\frac{\lambda_h^2 - 1}{\lambda_h} \right) x_- y_- \right] \\ \frac{dy_-}{dz_-} &= -\frac{1}{\lambda_h} x_-^2 (x_-^2 - y_-^2) + (x_-^2 + y_-^2 - 1) \left[-\beta + \beta y_-^2 + \frac{1}{\lambda_h} x_-^2 \right],\end{aligned}\quad (2.8)$$

where z_- is a new independent variable such that

$$\dot{z}_- = \sqrt{\frac{2\Lambda}{x_-^2 + y_-^2 - 1}}. \quad (2.9)$$

The unit circle is again an invariant set of the system, and the dynamics on this set is exactly the same as it was for the (x_+, y_+) coordinates.

We now have two new sets of variables, taking values in either the ‘plus’ plane or the ‘minus’ plane. The dynamics on the ‘plus’ plane incorporates the full dynamics on the (u, v) plane for $\Lambda > 0$, including trajectories ‘at infinity’ on this plane, and also the ‘large radius’ dynamics on the (u, v) plane for $\Lambda < 0$, again including trajectories ‘at infinity’. Conversely, the dynamics on the ‘minus’ plane incorporates the full dynamics for $\Lambda < 0$ and the ‘large radius’ dynamics for $\Lambda > 0$, again including trajectories ‘at infinity’. Taken together, the dynamics on the ‘plus’ and ‘minus’ planes incorporates the full dynamics for either sign of Λ , including the trajectories ‘at infinity’, which is mapped to the unit circle. The phase space for this dynamics is topologically a sphere. The (x_+, y_+) coordinates cover a connected open set that includes the whole of one ‘hemisphere’ while the (x_-, y_-) coordinates cover a connected open set that includes the whole of the other ‘hemisphere’. The overlap is an annular region containing the unit circle on either the (x_+, y_+) or (x_-, y_-) plane, and the two sets of coordinates on this region are related by

$$(x_+, y_+) = \frac{1}{\sqrt{2x_-^2 + 2y_-^2 - 1}} (x_-, y_-), \quad (x_-, y_-) = \frac{1}{\sqrt{2x_+^2 + 2y_+^2 - 1}} (x_+, y_+). \quad (2.10)$$

Note that this maps the unit circle to the unit circle. Note too that the line $x_+ = \pm 1/\sqrt{2}$ is mapped to the line $y_- = \pm 1/\sqrt{2}$, consistent with our earlier observation that the $k = 0$ trajectories consist of the lines $2x_+^2 = 1$ in the ‘plus’ plane and $2y_-^2 = 1$ in the ‘minus’ plane.

2.2 Fixed points

Having determined the global topology, we will find it more convenient to proceed in terms of the new variables (x, y) defined by

$$(x, y) = \frac{1}{\sqrt{u^2 + v^2 + 2|\Lambda|}} (u, v), \quad (u, v) = \sqrt{\frac{2|\Lambda|}{1 - x^2 - y^2}} (x, y). \quad (2.11)$$

These new variables coincide with (x_+, y_+) for $\Lambda > 0$ and with (x_-, y_-) for $\Lambda < 0$, which means that the dynamical system on the (u, v) plane is mapped into the interior of the unit circle for either sign of Λ . We thus have two dynamical systems defined in the unit disc in the (x, y) plane, and we distinguish between them according to the sign

$$\eta = \operatorname{sgn}\Lambda. \quad (2.12)$$

The equations for these two dynamical systems are

$$\begin{aligned} \frac{dx}{d\zeta} &= \frac{1}{2\alpha} xy (x^2 - y^2) + (x^2 + y^2 - 1) \left[\frac{\eta\lambda}{2} - \frac{\lambda}{2} (1 + \eta) x^2 + (\alpha - \eta\beta) xy \right] & (2.13) \\ \frac{dy}{d\zeta} &= \frac{1}{2\alpha} x^2 (y^2 - x^2) + (x^2 + y^2 - 1) \left[\beta\eta - \frac{\lambda}{2} (1 + \eta) xy + \beta (1 - \eta) y^2 + \frac{1}{2\alpha} x^2 \right], \end{aligned}$$

where ζ is a new independent variable such that

$$\dot{\zeta} = \sqrt{\frac{2|\Lambda|}{1 - x^2 - y^2}}. \quad (2.14)$$

The fixed points on the unit circle are clearly the same for both systems. As already observed, there are six such fixed points, which we consider in pairs, in each case giving both positions and the eigenvalues of the Jacobian matrices. Firstly, we have

- Two saddles

$$(0, 1) : \left\{ 2\beta, -\frac{1}{2\alpha} \right\}, \quad (0, -1) : \left\{ \frac{1}{2\alpha}, -2\beta \right\}. \quad (2.15)$$

Secondly, there are four $k = 0$ fixed points ‘at infinity’:

- Two nodes:

$$\pm \left(\frac{1}{\sqrt{2}}, -\frac{1}{\sqrt{2}} \right) : \mp\sqrt{2} \left\{ \frac{1}{2\alpha}, \frac{\lambda_h + \lambda}{2} \right\}. \quad (2.16)$$

- Two that are nodes for $\lambda < \lambda_h$ and saddles for $\lambda > \lambda_h$:

$$\pm \left(\frac{1}{\sqrt{2}}, \frac{1}{\sqrt{2}} \right) : \pm\sqrt{2} \left\{ \frac{1}{2\alpha}, \frac{\lambda_h - \lambda}{2} \right\}. \quad (2.17)$$

These two fixed points are non-hyperbolic when $\lambda = \lambda_h$.

From the global perspective, the last four fixed points are intersections of the great circle ‘at infinity’ on the spherical phase space with the continuous curve on the sphere defined by the combined $k = 0$ trajectories of the $\Lambda > 0$ and $\Lambda < 0$ systems. If the sphere is viewed as the surface of a tennis ball then this curve can be viewed as its seam.

The structure of trajectories inside the unit circle depends on the sign of Λ so we now consider these two cases separately:

2.2.1 $\Lambda < 0$

Setting $\eta = -1$ in (2.13) we have

$$\begin{aligned}\frac{dx}{d\zeta} &= \frac{1}{\lambda_h} (1 - 2y^2) xy + \frac{1}{2} (x^2 + y^2 - 1) (2\lambda_h xy - \lambda) , \\ \frac{dy}{d\zeta} &= \frac{1}{\lambda_h} (2y^2 - 1) [x^2 + \beta\lambda_h (x^2 + y^2 - 1)] .\end{aligned}\quad (2.18)$$

There are two types of ‘interior’ fixed point (i.e. inside the unit circle):

- Type (i), or $k = 0$, fixed points at

$$(x, y) = \pm \frac{1}{\sqrt{2}\lambda_h} (\lambda, \lambda_h) \quad (2.19)$$

These lie within the unit circle iff $\lambda < \lambda_h$. The eigenvalues of the Jacobian matrix at these fixed points are

$$\pm \frac{1}{2\sqrt{2}\lambda_h} \{ (\lambda^2 - \lambda_h^2), 2(\lambda^2 - \lambda_c^2) \} \quad (2.20)$$

This shows that these fixed points become non-hyperbolic at $\lambda = \lambda_c$ (where they coincide with the ‘type (ii)’ fixed points to be discussed below) and at $\lambda = \lambda_h$ (where they coincide with fixed points ‘at infinity’).

- Type (ii) fixed points at

$$(x, y) = \pm \frac{1}{\sqrt{\lambda^2 + \lambda_c^2}} (2\beta, \lambda) \quad (2.21)$$

The eigenvalues of the Jacobian matrix at these fixed points are

$$\pm \frac{1}{2\lambda_h \sqrt{\lambda^2 + \lambda_c^2}} \left\{ -\lambda + \sqrt{4\lambda_c^2(\lambda_c^2 - \lambda^2) + \lambda^2}, -\lambda - \sqrt{4\lambda_c^2(\lambda_c^2 - \lambda^2) + \lambda^2} \right\} \quad (2.22)$$

These fixed points are saddles for $\lambda < \lambda_c$, nodes for $\bar{\lambda} \leq \lambda > \lambda_c$ and foci for $\lambda > \bar{\lambda}$, where $\bar{\lambda} = 4\sqrt{(d-2)(d-10)}$. When $\lambda = \lambda_c$ they coincide with the type (i) fixed points.

2.2.2 $\Lambda > 0$

Setting $\eta = 1$ in (2.13) we have

$$\begin{aligned}\frac{dx}{d\zeta} &= \frac{1}{2\lambda_h} (2x^2 - 1) [2xy - \lambda\lambda_h (x^2 + y^2 - 1)] , \\ \frac{dy}{d\zeta} &= \frac{1}{\lambda_h} x^2 (2y^2 - 1) + (x^2 + y^2 - 1) (\beta - \lambda xy) .\end{aligned}\quad (2.23)$$

We may again classify fixed points into two types:

- Type (i), or $k = 0$, fixed points at

$$(x, y) = \pm \frac{1}{\sqrt{2}\lambda} (\lambda, \lambda_h) \quad (2.24)$$

These fixed points are inside the unit circle if $\lambda > \lambda_h$. Their eigenvalues are the same as those of the $k = 0$ fixed points for $\Lambda < 0$. Since $\lambda_h > \lambda_c$, these fixed points are always hyperbolic, except when $\lambda = \lambda_h$, in which case they coincide with fixed points ‘at infinity’.

- Type (ii) fixed points lie on the line $2\beta y = \lambda x$, which is mapped into itself by the map (2.10) that takes the exterior of the unit circle into the interior of the unit circle. The positions of any such fixed points are therefore given again by (2.21), as one may verify, but these fixed points are now outside the unit circle.

2.3 Bifurcations at infinity

Bifurcations of families of dynamical systems occur when fixed points coincide for some values of the parameters, leading to a non-hyperbolic fixed point at the bifurcation. There is a bifurcation in the $\Lambda < 0$ family of dynamical systems when $\lambda = \lambda_c$ because in this case the type (i) and type (ii) fixed points coincide. It was shown in [1] that this is a *transcritical* bifurcation, in which the stability properties of two fixed points are exchanged as they cross in parameter space.

Inspection of (2.17) shows that these fixed points at infinity are non-hyperbolic when $\lambda = \lambda_h$; this is because they then coincide with the type (i) fixed points, which move to infinity as λ approaches λ_h . We now show that this leads to another transcritical bifurcation. We first define new variables (\check{x}, \check{y}) by

$$x = \pm \frac{1}{\sqrt{2}} + \check{x} - \check{y}, \quad y = \pm \frac{1}{\sqrt{2}} + \check{y} \quad (2.25)$$

and we define the new parameter

$$s = \pm \frac{1}{\sqrt{2}} (\lambda - \lambda_h) . \quad (2.26)$$

We now find, for $\eta = -1$, that the system is described by the equations⁴

$$\begin{aligned}\frac{d\check{x}}{d\zeta} &= s\check{x} + \lambda_h\check{x}^2 + \frac{2}{\lambda_h}\check{y}[(1 + 2\beta\lambda_h)\check{x} - 2\check{y}] + C(\check{x}, \check{y}, s) \\ \frac{d\check{y}}{d\zeta} &= \frac{\sqrt{2}}{\lambda_h}\check{y} + \check{y}L(\check{x}, \check{y}) ,\end{aligned}\tag{2.27}$$

where C is a polynomial function at least cubic in its arguments, and L is a polynomial function that is at least linear in its arguments.

There is a fixed point at the origin of the (\check{x}, \check{y}) plane that becomes non-hyperbolic at $s = 0$. One now considers the ‘extended’ system in which s becomes a variable subject to the trivial equation $ds/d\zeta = 0$. This system has a fixed point at the origin and we are interested in the dynamics on the centre manifold through this fixed point. Because of the structure of the above equations, the equation for this ‘extended’ centre manifold is simply $y = 0$ through quadratic order, so the equation for the dynamics on the extended centre manifold to quadratic order is

$$\frac{d\check{x}}{d\zeta} = s\check{x} + \lambda_h\check{x}^2 .\tag{2.28}$$

After flipping the sign of the independent variable, this equation becomes a standard one for a transcritical bifurcation. We now present a selection of global phase portraits for representative values of the parameters. We show the two hemispheres separately, but it is clear from the above discussion how they can be glued together to form a topological sphere.

⁴The equations for $\eta = 1$ are slightly different but diffeomorphic and hence yield equivalent results.

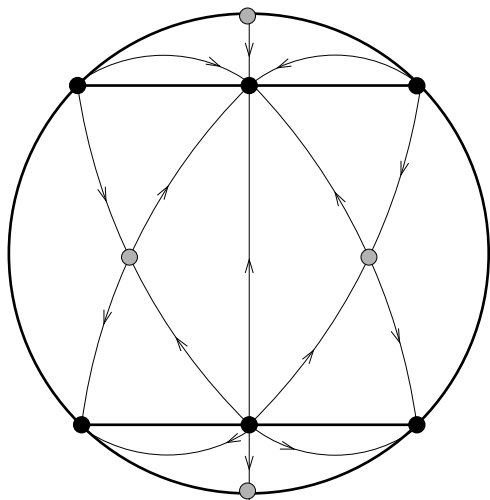


Figure 1: $\lambda = 0$. Hemisphere for $\Lambda < 0$.

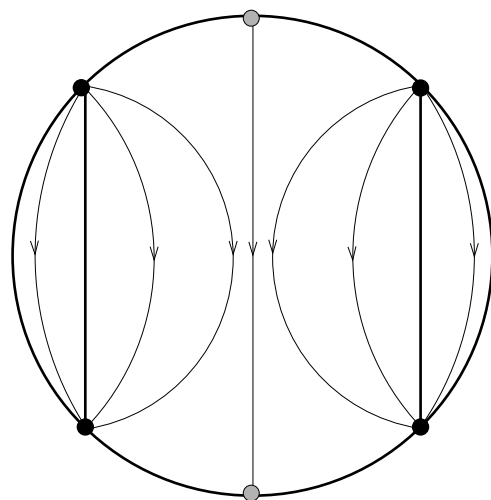


Figure 2: $\lambda = 0$. Hemisphere for $\Lambda > 0$.

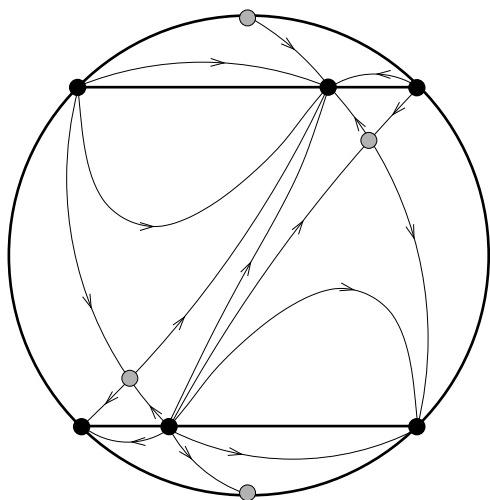


Figure 3: $\lambda < \lambda_c$. Hemisphere for $\Lambda < 0$.

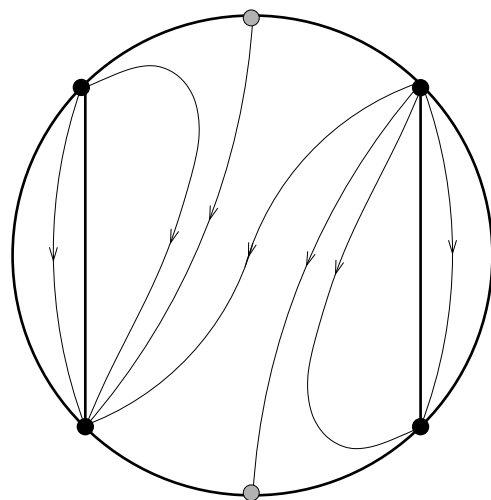


Figure 4: $\lambda < \lambda_c$. Hemisphere for $\Lambda > 0$.

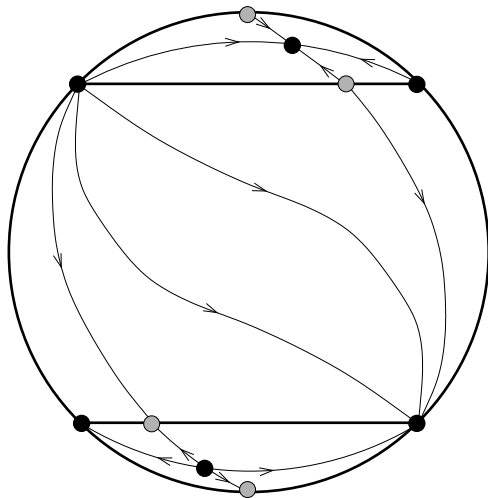


Figure 5: $\lambda_h > \lambda > \lambda_c$. Hemisphere for $\Lambda < 0$.

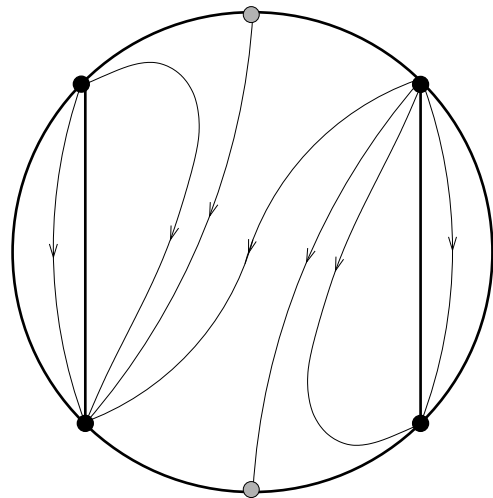


Figure 6: $\lambda_h > \lambda > \lambda_c$. Hemisphere for $\Lambda > 0$.

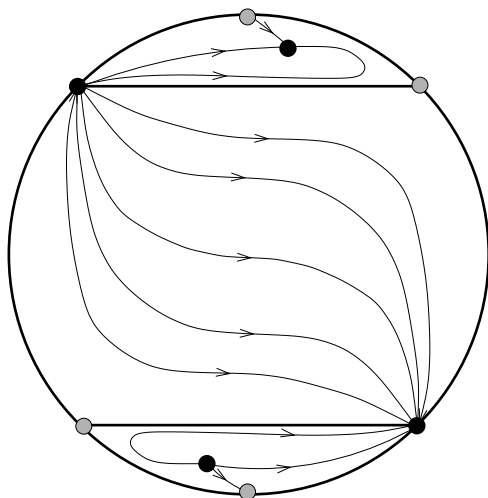


Figure 7: $\lambda > \lambda_h > \lambda_c$. Hemisphere for $\Lambda < 0$.

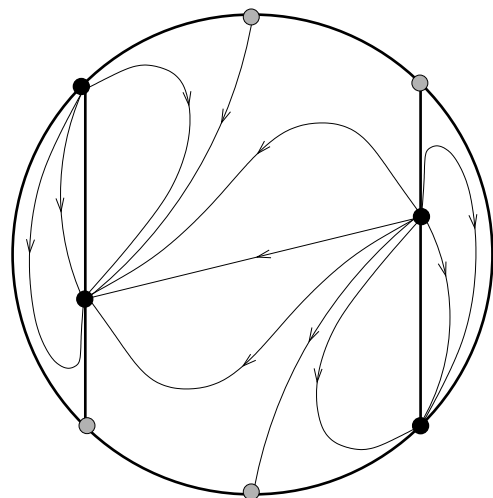


Figure 8: $\lambda > \lambda_h > \lambda_c$. Hemisphere for $\Lambda > 0$.

2.4 Trajectories vs solutions

For either sign of Λ the equations (2.1) are invariant under reflection through the origin

$$(u, v) \rightarrow -(u, v). \quad (2.29)$$

It follows that this transformation takes one trajectory into another trajectory, except for the trajectory through the origin, which is taken into itself. In particular, this explains why fixed points occur in pairs, since the origin is never a fixed point for non-zero Λ . This transformation is induced by the transformation $z \rightarrow -z$, so paired trajectories correspond to domain wall solutions that are related by this diffeomorphism, and $z \rightarrow -z$ must be an isometry of the solution corresponding to the trajectory through the origin.

These observations are nicely illustrated by the $\lambda = 0$ model with $\Lambda < 0$, for which all trajectories (in contrast to domain-wall solutions) are known exactly [1]. One finds that the two type (i) fixed points yield the metrics

$$ds_{\pm}^2 = dz^2 + e^{\pm 2\beta\sqrt{2|\Lambda|}z} ds^2(\mathbb{E}^{(1,d-2)}). \quad (2.30)$$

These are both locally adS metrics that are foliated by $(d-1)$ -dimensional Minkowski spaces. This foliation separates the entire adS spacetime into two regions⁵, separated by a Killing horizon, and each fixed point yields the metric on one of the two regions. The trajectory through the origin yields a solution with metric

$$ds^2 = dz^2 + \frac{1}{2\beta^2|\Lambda|} \cosh\left(\beta\sqrt{2|\Lambda|}z\right) ds^2(adS_{d-1}). \quad (2.31)$$

This is the same adS spacetime, but now foliated by $(d-1)$ -dimensional anti-de Sitter spaces. Note the $z \rightarrow -z$ isometry. Given global coordinates for the adS_{d-1} leaves of the foliation, the entire adS spacetime is now covered, including both regions covered by the fixed-point solutions. There are also two $k = 1$ trajectories that yield a metric that is locally adS, and these correspond to two regions of adS foliated by $(d-1)$ -dimensional de-Sitter (dS) spaces. These adS examples illustrate the further point that a given domain wall spacetime may be represented by more than one trajectory, if one regards as equivalent solutions that are locally diffeomorphic.

Another distinction between trajectories and solutions emerges when we consider $\lambda > 0$. It is particularly instructive to consider the models with

$$\lambda = \lambda_n \equiv \lambda_c \sqrt{\frac{n}{d+n-2}} \quad (2.32)$$

where n is a non-negative integer; note that $\lambda = 0$ for $n = 0$ and $\lambda_n < \lambda_c$. For $n \geq 1$, solutions of the Einstein-dilaton model lift to solutions of the $(d+n)$ -dimensional Einstein equations with cosmological constant Λ . Although the higher-dimensional solution will not necessarily have a domain-wall interpretation, the $k = 0$ fixed point solutions lift to the two Minkowski-foliated locally adS_{d+n} metrics that are separated

⁵By ‘adS’ we mean adS and not its covering space.

by a Killing horizon. These metrics do not cover the Killing horizon, which becomes a curvature singularity of the d -dimensional metric. However, the trajectory through the origin, which interpolates between the fixed points, yields a solution that lifts to a global covering of the adS_{d+n} spacetime, so this metric has a singularity at $z = 0$, so that the $z \rightarrow -z$ transformation now interchanges two singular metrics. It is natural to conjecture that the same result holds for all $\lambda < \lambda_c$, since the structure of trajectories is topologically the same as for $\lambda = 0$. Because of the bifurcation at $\lambda = \lambda_c$, there is a topology change for $\lambda > \lambda_c$ such that the trajectory through the origin now interpolates between $k = 0$ fixed points ‘at infinity’.

Another instructive example is provided by the $\lambda = \lambda_h$ model, for which there are just two $k = 0$ solutions, for either sign of Λ , given by⁶

$$e^{\lambda_h \varphi} = |z| \exp\left(-\frac{1}{4}\Lambda\lambda_h^2 z^2\right), \quad e^{\lambda_h \sigma} = |z|^{-1} \exp\left(-\frac{1}{4}\Lambda\lambda_h^2 z^2\right). \quad (2.33)$$

Consider the $\Lambda < 0$ case: then $\dot{\varphi} > 0$ for $z > 0$ and $\dot{\varphi} < 0$ for $z < 0$. These two possibilities correspond to the two $k = 0$ trajectories interchanged by the transformation $z \rightarrow -z$. Let us choose the $\dot{\varphi} > 0$ trajectory with $z > 0$, and set $\Lambda = -2/\lambda_h^2$ for simplicity. Then

$$e^{\lambda_h \varphi} = z e^{\frac{1}{2}z^2}, \quad e^{\lambda_h \sigma} = z^{-1} e^{\frac{1}{2}z^2} \quad (\Lambda = -2/\lambda_h^2) \quad (2.34)$$

and hence

$$\dot{\sigma} = z^{-1} (z^2 - 1). \quad (2.35)$$

We see that $\dot{\sigma} = 0$ at $z = 1$, so that the range of the function $\sigma(z)$ is restricted to

$$\sigma(z) \geq \sigma_{min} \equiv \sigma(1) = \frac{1}{2\lambda_h}. \quad (2.36)$$

The relation of z to the affine parameter \tilde{z} is found by integration of

$$d\tilde{z} = \frac{e^{\frac{1}{4}z^2}}{\sqrt{z}} dz \quad (2.37)$$

We see that $\tilde{z} \sim 2\sqrt{z}$ near $z = 0$. Thus the singularity of the metric and scalar field at $z = 0$ is at finite affine distance. The domain wall solution in this case is singular. Nevertheless, it will be useful later.

3 Flat walls

For $k = 0$ we have the dynamical system

$$\begin{aligned} \dot{u} &= -\alpha uv + \frac{1}{2}(\lambda - \mu)(u^2 - 2\Lambda) + \frac{1}{2}\mu v^2, \\ \dot{v} &= -\alpha v^2 + \frac{1}{2}\lambda uv - 2\alpha\Lambda \end{aligned} \quad (3.1)$$

⁶This solution was given in [1] but only for $z > 0$.

The constraint is

$$\dot{\chi}^2 = e^{-\mu\sigma} [v^2 - u^2 + 2\Lambda] , \quad (3.2)$$

and it implies that we must restrict the phase space by the inequality

$$v^2 - u^2 + 2\Lambda \geq 0 . \quad (3.3)$$

Note that when $v^2 - u^2 + 2\Lambda = 0$, the system reduces to the $k = 0$ case of the purely dilaton model, so the $k = 0$ trajectories of that model are the $\dot{\chi} = 0$ trajectories of the axion-dilaton model.

We record here that the spacetime metric for the gauge choice (1.6) used to obtain these equations is

$$ds^2 = e^{\lambda\sigma} dz^2 + e^{2\beta\varphi} ds^2 (\mathbb{E}^{(1,d-2)}) . \quad (3.4)$$

3.1 Global Structure and Fixed Points

Define the new coordinates

$$(X, Y) = \frac{1}{\sqrt{2v^2 + u^2 + 2\Lambda}} (u, v) , \quad (u, v) = \sqrt{\frac{2\Lambda}{1 - X^2 - 2Y^2}} (X, Y) \quad (3.5)$$

The physical region $v^2 - u^2 + 2\Lambda \geq 0$ is mapped onto the the interior of an ellipse:

$$2X^2 + Y^2 \leq 1 . \quad (3.6)$$

This ellipse can be identified with the $k = 0$ ‘tennis ball seam’ of the global phase space for constant axion trajectories described in the previous section.

The trajectories ‘at infinity’ in the (u, v) plane are mapped to the intersection with the physical region of the orthogonal ellipse

$$X^2 + 2Y^2 = 1 . \quad (3.7)$$

The physical region contains (i) the region with $X^2 + 2Y^2 < 1$, which is the phase space for $\Lambda > 0$, and (ii) two disjoint regions with $X^2 + 2Y^2 > 1$, which collectively form the phase space for $\Lambda < 0$. The equations in the new variables are

$$\begin{aligned} \frac{dX}{d\zeta} &= \frac{1}{2}\mu(1 - X^2)(1 - 2X^2 - Y^2) + \frac{1}{2}(1 - X^2 - 2Y^2)[\lambda_h XY - \lambda(1 - 2X^2)] \\ \frac{dY}{d\zeta} &= -\frac{1}{2}\mu XY(1 - 2X^2 - Y^2) + \frac{1}{2}(1 - X^2 - 2Y^2)[2\lambda XY - \lambda_h(1 - Y^2)] \end{aligned} \quad (3.8)$$

where ζ is a new independent variable such that

$$\dot{\zeta} = \sqrt{\frac{2\Lambda}{1 - X^2 - 2Y^2}} . \quad (3.9)$$

Observe that the boundary of the physical region, $X^2 + 2Y^2 = 1$ is an invariant set, and also that the two segments of the ellipse $2X^2 + Y^2 = 1$ within the physical region are invariant sets.

3.1.1 Boundary fixed points

There are two types of fixed point on the $2X^2 + Y^2 = 1$ boundary

- Fixed points ‘at infinity’: there are two fixed points on the ellipse, at $(X, Y) = (\pm 1, 0)$, but these are outside the physical region. The only fixed points ‘at infinity’ that are inside the physical region are also on the boundary of the physical region. There are four of them, and their positions and eigenvalues are as follows:

$$\begin{aligned} \pm \frac{1}{\sqrt{3}} (1, 1) : & \quad \left\{ -\frac{1}{\sqrt{3}}\mu, -\frac{1}{\sqrt{3}}(\lambda - \lambda_h) \right\} \\ \pm \frac{1}{\sqrt{3}} (1, -1) : & \quad \left\{ -\frac{1}{\sqrt{3}}\mu, -\frac{1}{\sqrt{3}}(\lambda + \lambda_h) \right\} \end{aligned} \quad (3.10)$$

- Apart from the boundary fixed points ‘at infinity’, there is another pair of fixed points on the boundary provided that $\lambda \neq \lambda_h$. These lie on the intersection of the boundary with the line $\lambda_h X = \lambda Y$. They have positions and eigenvalues

$$\pm \frac{1}{\sqrt{2\lambda^2 + \lambda_h^2}} (\lambda, \lambda_h) : \quad \left\{ \frac{\lambda^2 - \lambda_h^2}{2\sqrt{2\lambda^2 + \lambda_h^2}}, \frac{\lambda^2 - \lambda_h^2 - \mu\lambda}{\sqrt{2\lambda^2 + \lambda_h^2}} \right\} \quad (3.11)$$

If $\lambda < \lambda_h$ then these fixed points are on the boundary of the $\Lambda > 0$ region. If $\lambda > \lambda_h$ then there is one on each boundary of the two disjoint $\Lambda < 0$ regions. At $\lambda = \lambda_h$ these fixed points coincide with boundary fixed points ‘at infinity’.

3.1.2 Interior fixed points

There are a pair of fixed points with positions

$$(X, Y) = \pm \Delta^{-1} (\lambda_h, \lambda - \mu) . \quad (3.12)$$

where

$$\Delta = \sqrt{(\lambda - \mu)^2 + \lambda(\lambda - \mu) + \lambda_h^2} . \quad (3.13)$$

These are in the allowed region $2X^2 + Y^2 \leq 1$ provided that

$$\lambda(\lambda - \mu) \geq \lambda_h^2 . \quad (3.14)$$

Note that this condition requires $\lambda \geq \mu$, and that it is equivalent, for non-zero λ , to

$$\mu \leq \mu_c \equiv \frac{\lambda^2 - \lambda_h^2}{\lambda} . \quad (3.15)$$

These fixed points coincide with fixed points on the boundary when the inequality is saturated. When it is otherwise satisfied, there are two ‘interior’ fixed points, in the $\Lambda > 0$ region when $\mu > 0$, and one in each of the two $\Lambda < 0$ regions when $\mu < 0$.

The eigenvalues E_{\pm} of the Jacobian matrix at an interior fixed point are

$$\begin{aligned} E_1 &= \pm \frac{1}{4\Delta} \left\{ \mu\lambda_h + \sqrt{8\mu\lambda(\lambda - \mu)^2 - \mu(8\lambda - 9\mu)\lambda_h^2} \right\}, \\ E_2 &= \pm \frac{1}{4\Delta} \left\{ \mu\lambda_h - \sqrt{8\mu\lambda(\lambda - \mu)^2 - \mu(8\lambda - 9\mu)\lambda_h^2} \right\}. \end{aligned} \quad (3.16)$$

Note that

$$2\Delta^2 E_1 E_2 = -\mu(\lambda - \mu) [\lambda^2 - \lambda_h^2 - \mu\lambda]. \quad (3.17)$$

The last factor in this expression is necessarily positive for an interior fixed point, so the Poincaré index is -1 for $\mu > 0$ and $+1$ for $\mu < 0$. Index considerations therefore allow limit cycles only for $\mu < 0$. However, $\mu < 0$ corresponds to $\Lambda < 0$, and in this case the constraint (3.3) implies that φ is a monotone function, so limit cycles are excluded.

3.2 Bifurcations

As shown by (3.17), the pair of ‘internal’ fixed points are non-hyperbolic when $\mu\lambda = \lambda^2 - \lambda_h^2$, which is equivalent to $\mu = \mu_c$. Recall that $\mu \leq \mu_c$ was the condition for the ‘internal’ fixed points to lie within the allowed region, so when $\mu = \mu_c$ they have moved to the boundary of the allowed region, where they coincide with the boundary fixed points of (3.11). Here we study the nature of the bifurcation as the curve $\mu = \mu_c(\lambda)$ is crossed in the (λ, μ) plane (Fig. 9).

Without loss of generality we may concentrate on the pair of fixed point in the $Y > 0$ region, and we define new variables (\check{X}, \check{Y}) by

$$X = \frac{\lambda}{\sqrt{\lambda_h^2 + 2\lambda^2}} - \frac{\lambda_h}{2\lambda} \check{X} - \frac{\lambda^2 + 2\lambda_h^2}{3\lambda\lambda_h} \check{Y}, \quad Y = \frac{\lambda_h}{\sqrt{\lambda_h^2 + 2\lambda^2}} + \check{X} + \check{Y}. \quad (3.18)$$

The fixed point is now at the origin in the (\check{X}, \check{Y}) plane. We are interested in the behaviour for $\mu \approx \mu_c(\lambda)$, so we also define

$$s = \frac{\lambda(\mu - \mu_c)}{\sqrt{\lambda_h^2 + 2\lambda^2}}. \quad (3.19)$$

The equations of the dynamical system near the origin in $(\check{X}, \check{Y}, s)$ space take the form

$$\frac{d\check{X}}{d\zeta} = \frac{\lambda^2 - \lambda_h^2}{2\sqrt{\lambda_h^2 + 2\lambda^2}} \check{X} + Q_1(\check{X}, \check{Y}; s), \quad \frac{d\check{Y}}{d\zeta} = s \check{Y} + Q_2(\check{X}, \check{Y}; s), \quad (3.20)$$

together with the trivial equation $s' = 0$. The functions Q_1 and Q_2 are polynomials in (\check{X}, \check{Y}) that are at least quadratic in these variables, with coefficients that may depend on s . For our purposes, the relevant terms are

$$Q_1 = \frac{13\lambda_h^2 - \lambda^2}{9\lambda_h} \check{Y}^2 + \dots, \quad Q_2 = -\frac{2\lambda_h(\lambda_h^2 + 2\lambda^2)}{3\lambda^2} \check{Y}^2 + \dots \quad (3.21)$$

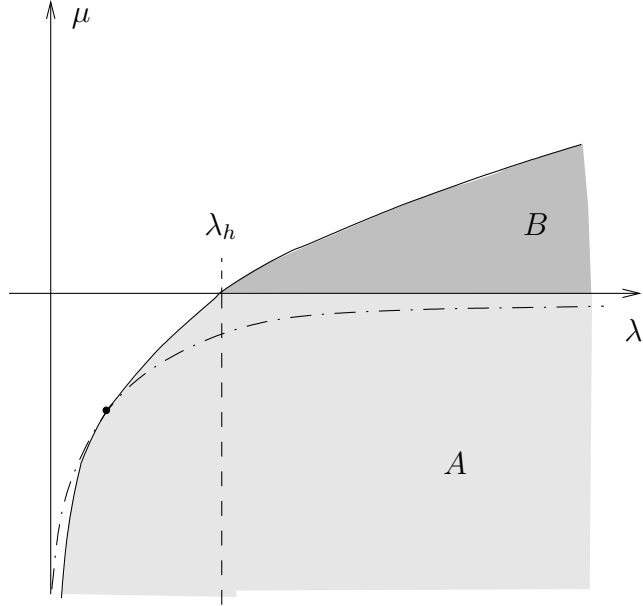


Figure 9: The (μ, λ) plane. For parameter values inside the semi-infinite grey region $A \cup B$ there exist internal fixed points. The curve bounding this region from above is given by the equation $\lambda\mu = \lambda^2 - \lambda_h^2$, i.e. $\mu = \mu_c$. For $\mu < 0$ (A) these are located in the two $\Lambda < 0$ regions and for $\mu > 0$ (B) they are in the $\Lambda > 0$ region. The dash-dotted lines indicate the curve $\mu\lambda = -2$ in relation to the curve $\mu = \mu_c$ for $d = 4$.

The equation for the centre manifold of this system (i.e. the ‘extended’ centre manifold) is, to quadratic order,

$$\ddot{X} = -\frac{2\sqrt{\lambda_h^2 + 2\lambda^2}(13\lambda_h^2 - \lambda^2)}{9\lambda_h(\lambda^2 - \lambda_h^2)}\ddot{Y}^2 + \dots \quad (3.22)$$

Evidently, we must assume that $\lambda \neq \lambda_h$, since in this case there is a coincidence of three fixed points and the bifurcation is more complicated. The dynamics for the evolution on the extended centre manifold is governed by the equation

$$\frac{d\ddot{Y}}{d\zeta} = s\ddot{Y} - \frac{2\lambda_h(\lambda_h^2 + 2\lambda^2)}{3\lambda^2}\ddot{Y}^2 + \dots \quad (3.23)$$

From this formula it is evident that the bifurcation is transcritical.

There is a much more complicated bifurcation at $\mu = 0$. Again we restrict to $\lambda \neq \lambda_h$. In this case, equations (3.8) imply that the two segments of the ellipse $X^2 + 2Y^2 = 1$ inside the physical region become lines of fixed points. The shape of the trajectories follows from the differential equation

$$\frac{dY}{dX} = \frac{2\lambda XY - \lambda_h(1 - Y^2)}{\lambda_h XY - \lambda(1 - 2X^2)}, \quad (3.24)$$

which has the solution

$$c(\lambda Y - \lambda_h X)^2 = 1 - Y^2 - 2X^2, \quad (3.25)$$

for constant c . Trajectories inside the physical region have $c \geq 0$, and $c = 0$ corresponds to the boundary ellipse. All trajectories are segments of some ellipse that passes through the fixed points on the intersection of the boundary with the line $\lambda_h X = \lambda Y$. These fixed points are in the $\Lambda < 0$ regions if $\lambda < \lambda_h$ (Fig. 11) and in the $\Lambda > 0$ region if $\lambda > \lambda_h$ (Fig. 15). If $\lambda > \lambda_h$, then $\mu_c(\lambda) > 0$, so that $\mu < \mu_c$ at the bifurcation. In this case each $\Lambda < 0$ region is bounded by a heteroclinic cycle, and this leads to the quasi-cyclical $\Lambda < 0$ trajectories of Fig. 14.

As μ approaches zero, the interior fixed point approaches the line at infinity and merges with it at $\mu = 0$; there this line turns into a line of fixed points. The physical trajectories are segments of ellipses (3.25) emanating from the boundary fixed points on either side of the $\dot{\chi} = 0$ boundary of the $\Lambda > 0$ region (Fig. 15). There is a unique ellipse, with $1/c = \lambda^2 - \lambda_h^2$, which just grazes the two boundaries at infinity (indicated by a dashed line in Fig. 15); it touches them precisely at the limiting position of the interior fixed point as $\mu \rightarrow 0$. Furthermore, the location of this fixed point at $\mu = 0$ divides the lines at infinity into two regions. Concentrating on the $Y > 0$ case, we have a line of repellers to the left of the fixed point and a line of attractors to the right, making this line a kind of extended saddle. As μ becomes negative, the interior fixed point wanders into the $\Lambda > 0$ region where it becomes a proper saddle. The drastic change in the topology of the flow is illustrated in Figs. 14, 15 and 16. If $\lambda < \lambda_h$, there is no interior fixed point in the physical region as μ goes through zero. The corresponding bifurcation is illustrated in Figs. 10 - 12. At $\mu = 0$ the trajectories are again given by segments of ellipses (3.25), now emanating from the boundary fixed points in the $\Lambda < 0$ regions. The two lines ‘at infinity’ are again lines of fixed points. There is now a universal repeller in the $Y > 0$ region and a universal attractor in the $Y < 0$ region.

3.3 An exact axion-dilaton domain-wall solution

The interior fixed point solution has

$$(u, v) = \pm A(\lambda_h, \lambda - \mu), \quad e^{\frac{1}{2}\mu\sigma}\dot{\chi} = \left(\frac{\mu\lambda_h}{2}\right)\kappa A \quad (3.26)$$

where

$$A = \sqrt{\frac{2\Lambda}{\mu(\lambda - \mu)}}, \quad |\kappa| = \frac{2}{\lambda_h}\sqrt{\frac{\lambda(\mu_c - \mu)}{\mu^2}}. \quad (3.27)$$

Recall that the existence of an interior fixed point requires that both $\lambda - \mu$ and Λ/μ be positive, and that $\mu < \mu_c$, so that the constants A and κ are real.

Integrating the equations $\dot{\sigma} = u$ and $\dot{\varphi} = \varphi$, we obtain the following new exact domain-wall solution

$$\sigma = \pm\lambda_h A(z - z_0), \quad \varphi = \pm(\lambda - \mu)A(z - z_0) + \varphi_0, \quad (3.28)$$

where z_0 and φ_0 are integration constants, and χ is such that

$$e^{\frac{1}{2}\mu\sigma}(\chi - \chi_0) = \kappa, \quad (3.29)$$

where χ_0 is a further integration constant.

The spacetime metric for a convenient choice of φ_0 is

$$ds^2 = d\rho^2 + \rho^{4\beta/\lambda} ds^2(\mathbb{E}^{(1,d-2)}) , \quad (3.30)$$

where

$$\rho = \pm \frac{2}{\lambda \lambda_h A} \exp \left(\pm \frac{\lambda \lambda_h}{2} A(z - z_0) \right) . \quad (3.31)$$

This solution will play an important role in the discussion of supersymmetry to follow.

Although the limiting case in which $\mu = \mu_c$ yields a solution with constant axion, this case is of interest because the $\mu = \mu_c$ models include the $d = 4$ Freedman-Schwarz (FS) supergravity theory, which has a supersymmetric domain wall solution [17]. In fact, the above solution generalizes the FS domain-wall to any d when $\mu = \mu_c$. More significantly, it shows that the further generalization to $\mu < \mu_c$ requires a non-constant axion field. We now present a selection of global phase portraits for representative values of the parameters.

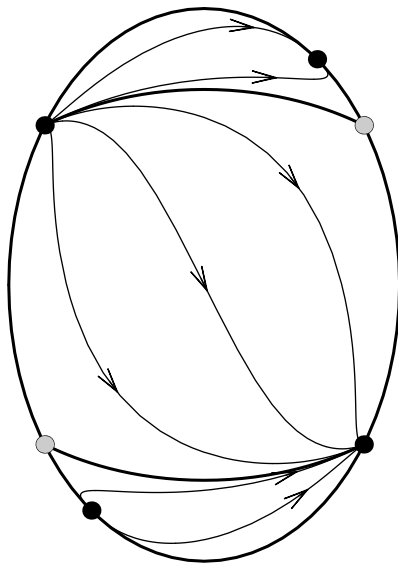


Figure 10: $\lambda < \lambda_h$; $\mu > 0$. There are no fixed points in the interior of the allowed region. Saddles are grey dots, nodes black dots.

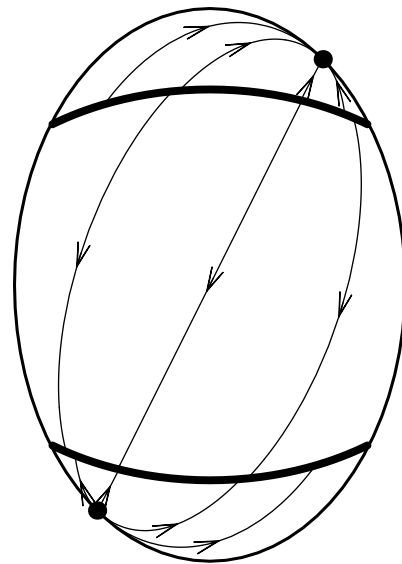


Figure 11: $\lambda < \lambda_h$; $\mu = 0$. The segments of the orthogonal ellipse at infinity turn into lines of fixed points on which there is no flow.

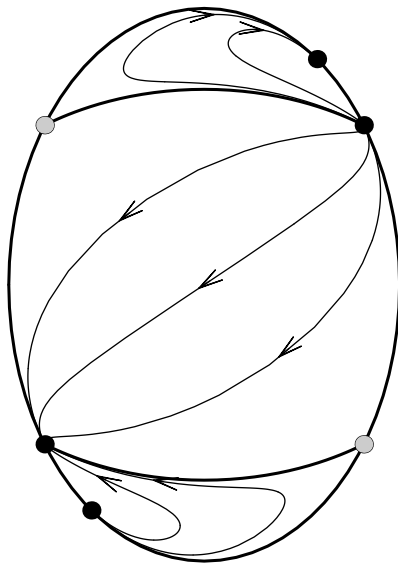


Figure 12: $\lambda < \lambda_h$; $\mu_c < \mu < 0$.

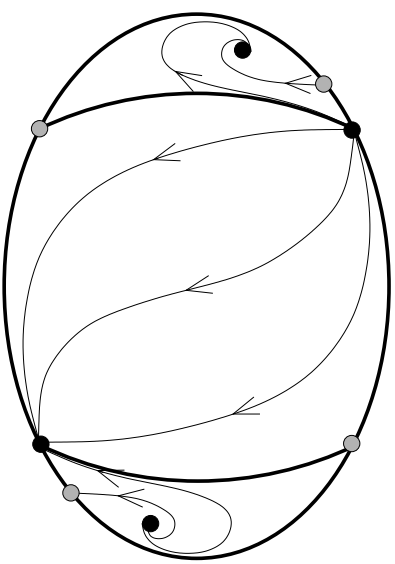


Figure 13: $\lambda < \lambda_h$; $\mu < \mu_c < 0$. There is now a fixed point inside the physical region.

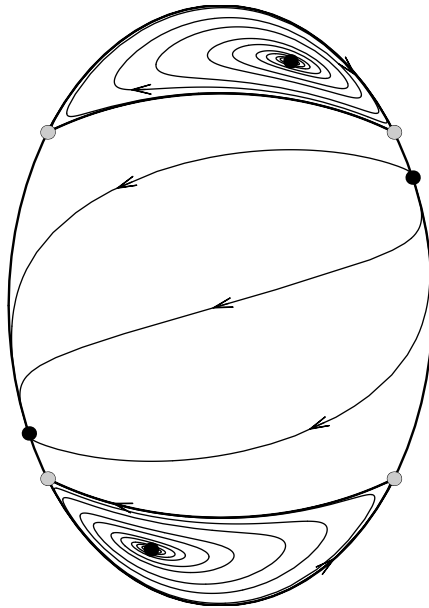


Figure 14: $\lambda > \lambda_h$; $\mu < 0$. Note the quasi-cyclical behaviour in the $\Lambda < 0$ regions.

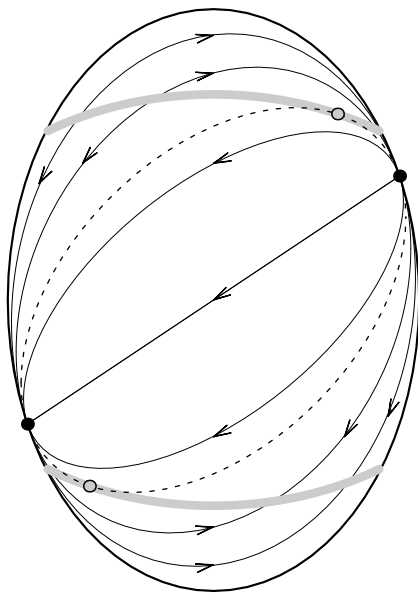


Figure 15: $\lambda > \lambda_h$; $\mu = 0$. The segments of the orthogonal ellipse at infinity turn into lines of fixed points on which there is no flow.

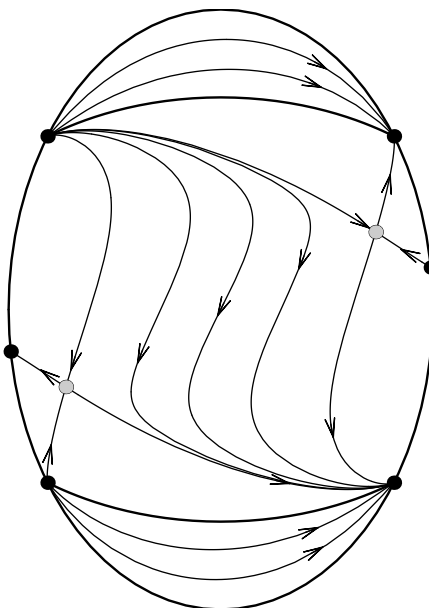


Figure 16: $\lambda > \lambda_h$; $\mu_c > \mu > 0$.

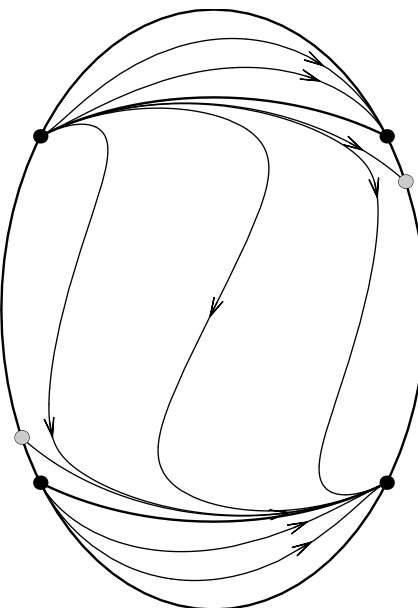


Figure 17: $\lambda > \lambda_h$; $\mu > \mu_c > 0$.

4 Supersymmetry

For domain wall solutions of supergravity theories it is of interest to ask of any given solution whether it is supersymmetric, since supersymmetry implies stability. A necessary condition for a domain wall solution to be supersymmetric is that it admit a Killing spinor, and this condition is also sufficient for models with only a single scalar field, e.g. a dilaton field, because the vanishing of the dilatino supersymmetry variation is then an integrability condition for the existence of a Killing spinor. Another simplifying feature of single-scalar models is that both the potential V and the Killing spinor equation are determined by a ‘superpotential’ alone; in the multi-scalar case there is an additional dependence on the target space metric. An example of a single scalar supergravity model is minimal $d = 3$ supergravity coupled to a scalar multiplet. In this case the superpotential is a real function $W(\sigma)$ of the single scalar field σ and the potential is given in terms of W by the formula

$$V = 2 \left[(W')^2 - \alpha^2 W^2 \right], \quad (4.1)$$

where the prime indicates a derivative with respect to σ . This formula can be immediately generalized to d dimensions, as is implicit in the way it has been written. The analogous d -dimensional generalization of the Killing spinor equation is

$$\left[D_\mu - \frac{1}{2(d-2)} W \Gamma_\mu \right] \epsilon = 0. \quad (4.2)$$

In the $d = 3$ supergravity context this equation arises from the requirement of vanishing supersymmetry variation of the gravitino field, in which case ϵ is an anticommuting spinor parameter, but linearity of the equation allows us to re-interpret it as a commuting spinor field, now on a d -dimensional spacetime.

The point of this generalization to arbitrary d of the notion of a supersymmetric domain wall solution of $d = 3$ supergravity is that domain walls admitting Killing spinors with respect to some superpotential W will be classically stable even when there is no underlying supergravity theory, although stability against non-perturbative tunnelling to some lower-energy configuration is not precluded. This state of affairs is described by saying that W defines a ‘fake’ supergravity theory. Its ‘fake’ supersymmetric domain wall solutions satisfy

$$f^{-1} \dot{\varphi} = \mp 2\alpha e^{\alpha\varphi} W, \quad f^{-1} \dot{\sigma} = \pm 2e^{\alpha\varphi} W', \quad (4.3)$$

because any solution of these equations is a flat domain wall solution of the second-order equations for (φ, σ) , and of the diffeomorphism constraint, such that the domain wall metric admits a Killing spinor. A fake supersymmetric domain-wall may be genuinely supersymmetric if the superpotential arises in the context of some ‘genuine’ supergravity theory with the required bosonic truncation, such that (i) the potential takes the form (4.1) and (ii) the condition of vanishing supersymmetry variation of the gravitino field reduces to (4.2). The conditions under which this happens for $d = 5$ supergravity were investigated in [16], and we will determine here the conditions under

which this happens for $d = 4$ supergravity. When there is an underlying supergravity theory we shall say that the domain wall solution is ‘genuinely’ supersymmetric, and we will usually omit the adjective ‘fake’ that should qualify the generic case because this should be clear from the context.

Only special solutions can be supersymmetric with respect to a *given* superpotential W , but almost any flat domain wall determines a superpotential W with respect to which it is supersymmetric [4, 1, 5]. The proof is by construction of W . Given $\varphi(z)$ and a choice of the function f , the first of equations (4.3) determines W as a function of z . Then, given $\sigma(z)$, the inverse function $z(\sigma)$ yields W as a function of σ , and one may verify that $W(\sigma)$ so defined yields the potential according to the formula (4.1). A complex superpotential is needed for the same statement to be true of curved walls, but we shall restrict our attention to flat domain walls, for which a real superpotential suffices. The qualification ‘almost’ arises because the function $z(\sigma)$ is defined only when $\sigma(z)$ is strictly monotonic, i.e. only when $\dot{\sigma} \neq 0$. This monotonicity condition fails for adS vacua, viewed as domain walls, because these have $\sigma \equiv 0$; this is expected because adS vacua may be unstable. It also fails for domain walls that are asymptotic to an unstable adS vacuum because in this case the asymptotic solution is an accumulation point for zeros of $\dot{\sigma}$ [14].

We will begin our investigation of domain wall supersymmetry by examining in more detail what happens at an isolated zero of $\dot{\sigma}$. We will confirm the ‘piecewise supersymmetry’ conclusion of [5] but the details are instructive and suggest a general picture that we elaborate in the context of asymptotically adS domain walls. Then we turn to a consideration of supersymmetry in multi-scalar models, using the axion-dilaton models as a ‘laboratory’. The exact solution of subsection 3.3 is useful in this respect and what we learn from it motivates a new multi-scalar extension of the ideas of fake supergravity.

4.1 Single-scalar models revisited

The formula (4.1) implies that

$$V' = 4W' (W'' - \alpha^2 W) . \quad (4.4)$$

It is usually concluded that stationary points of W are stationary points of V , with $V < 0$, but this assumes that W'' is non-singular when $W' = 0$. It may happen that a zero of W' is cancelled by a pole of W'' such that V' is finite and non-zero. We shall argue here that this possibility is realized for any superpotential constructed from a solution for which $\dot{\sigma}$ has an isolated zero. Rather than present a general proof we illustrate the point with two examples, one explicit and the other implicit. The explicit example arises from an exact domain-wall solution of the $\lambda = \lambda_h$ Einstein-dilaton model, for which $\dot{\sigma}$ has a single isolated zero [1]. The implicit example arises in the context of asymptotically adS domain walls.

Before proceeding we pause to discuss some consequences of the choice of the function f in (4.3). For the choice made in (1.6), which coincides with the choice

made in [1], the first-order equations (4.3) become

$$\dot{\varphi} = \mp \lambda_h e^{\frac{1}{2}\lambda_h \sigma} W, \quad \dot{\sigma} = \pm 2e^{\frac{1}{2}\lambda_h \sigma} W'. \quad (4.5)$$

The choice $f = e^{-\alpha\varphi}$, which was made in [5], leads to simpler first-order equations in terms of an affine distance variable, which we called \tilde{z} in subsection 1.1. In terms of this affine distance variable, defined as a function of z by (1.11) the equations (4.5) become

$$\dot{\varphi} = 2\alpha W, \quad \dot{\sigma} = -2W'. \quad (4.6)$$

where the grave accent indicates differentiation with respect to \tilde{z} .

4.1.1 Branched superpotentials

Let us first return to the domain wall solution of the $\lambda = \lambda_h$ constant axion model with $\Lambda = -2/\lambda_h^2$ studied in subsection 2.4. Recall that $\dot{\sigma}(z)$ has a zero at $z = 1$ for this solution. Our aim is to elucidate the implication of this fact for supersymmetry. Using the solution to construct a superpotential in the way just reviewed, one finds that

$$W(\sigma) = \mp \left(\frac{1 + \lambda_h^2 z^2}{\lambda_h^2 z} \right) e^{-\frac{1}{2}\lambda_h \sigma}, \quad (4.7)$$

where $z(\sigma)$ is determined implicitly by

$$e^{\lambda_h \sigma} = z^{-1} e^{\frac{1}{2}z^2}. \quad (4.8)$$

Observe that $z' = z/(z^2 - 1)$, and hence that

$$W' = \mp \left(\frac{1 - z^2}{2z} \right) e^{-\frac{1}{2}\lambda_h \sigma}. \quad (4.9)$$

We see that W' vanishes at $z = 1$, i.e. at $\sigma = \sigma_{min} \equiv \sigma(1)$. On the one hand, this is required by the second of equations (4.5), since $\dot{\sigma} = 0$ at $z = 1$. On the other hand, the absence of any stationary points of V would lead us to expect the same of W . This apparent contradiction is resolved by the observation that

$$W'' - \alpha^2 W = \mp \left(\frac{\lambda_h z}{1 - z^2} \right) e^{-\frac{1}{2}\lambda_h \sigma}. \quad (4.10)$$

This diverges precisely when $W' = 0$, such that

$$4W' [W'' - \alpha^2 W] \equiv 2\lambda_h e^{-\lambda_h \sigma} \equiv V', \quad (4.11)$$

as expected. This illustrates the important point that *stationary points of W are not necessarily stationary points of V* .

The superpotential of (4.7) is defined only for $\sigma > \sigma_{min}$. This is not a problem *per se* because the solution is such that $\sigma \geq \sigma_{min}$, but the minimum of $\sigma(z)$ is a branch point of the function $z(\sigma)$. The same is therefore true of $W(\sigma)$. In fact, one has

$$W(\sigma) \sim W_0 |\sigma - \sigma_{min}|^{\frac{3}{2}} \quad \text{as } \sigma \rightarrow \sigma_{min} \quad (4.12)$$

for constant W_0 , implying that $W(\sigma)$ is double-valued with a branch point at $\sigma = \sigma_{min}$. As z varies through 1, the function $W(\sigma)$ switches from one branch to the other. In other words, the solution is ‘piecewise supersymmetric’.

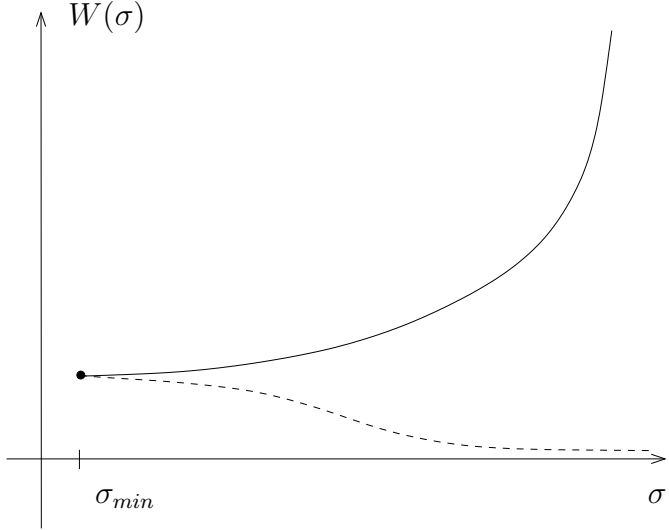


Figure 18: The branched superpotential. One branch is shown as a solid line, the other branch is shown as a dashed line. Both branches are defined for all $\sigma \geq \sigma_m$.

4.1.2 Asymptotically adS walls

We now move on to more general potentials $V(\sigma)$. Of particular interest, and common occurrence in supergravity models, are potentials with stationary points of V at which $V < 0$. These yield adS vacua. Given such a stationary point at $\sigma = 0$, the potential has the expansion

$$V = -\frac{1}{2\beta^2\ell^2} + \frac{1}{2}m^2\sigma^2 + \dots \quad (4.13)$$

where ℓ is the adS radius and m the mass of the σ -particle in this vacuum. The vacuum will be perturbatively stable as long as m^2 satisfies the d -dimensional Breitenlohner-Freedman (BF) bound [18, 19]

$$m^2 \geq -\frac{(d-1)^2}{4\ell^2} \equiv m_{BF}^2. \quad (4.14)$$

For a domain wall (flat or curved) that is asymptotic to the adS vacuum as $\tilde{z} \rightarrow \infty$, one has [14]

$$\sigma \sim e^{-\nu\tilde{z}/\ell}, \quad \dot{\varphi} \sim \frac{1}{\beta\ell} + \frac{\alpha\nu}{2\ell}e^{-2\nu\tilde{z}/\ell}, \quad (4.15)$$

where ν is a real positive root of the quadratic function $\nu^2 - (d-1)\nu - m^2\ell^2$. The roots

$$\nu_{\pm} = \frac{1}{2} \left[d-1 \pm \sqrt{(d-1)^2 + 4m^2\ell^2} \right], \quad (4.16)$$

are real as long as the BF bound is satisfied, and if $m^2 < 0$ then both ν_+ and ν_- are positive. If $m^2 \geq 0$ then only ν_+ is positive.

If we use the asymptotic solution (4.15) for $\nu = \nu_{\pm}$ to construct the superpotential with respect to which it is supersymmetric then we may assume that $W \geq 0$ at $\sigma = 0$

without loss of generality because the overall sign of W serves only to distinguish between walls and ‘anti-walls’. One finds the superpotential

$$W_{\pm} = \frac{1}{2\alpha\beta\ell} + \frac{\nu_{\pm}}{4\ell}\sigma^2 + \dots \quad (4.17)$$

The construction guarantees that this solves (4.1), as one may verify, although we actually find the W_- superpotential this way only for $m^2 > 0$ because for $m^2 \leq 0$ there is no domain wall associated with W_- because ν_- is not positive⁷. There is a further one-parameter family of perturbative solutions W_M of (4.1) with the expansion

$$W_M(\sigma) = \sqrt{M^2 + \frac{(d-2)^2}{\ell^2}} + \alpha M\sigma + \frac{1}{2}\alpha^2 \sqrt{M^2 + \frac{(d-2)^2}{\ell^2}}\sigma^2 + \dots \quad (4.18)$$

where M must be non-zero since the coefficient of the σ^3 term diverges as $M \rightarrow 0$, but is otherwise an arbitrary real number. Domain walls that are supersymmetric with respect to W_M are not asymptotic to the adS vacuum at $\sigma = 0$.

To summarize, each perturbatively-stable adS vacuum is associated with two superpotentials W_{\pm} that are stationary at the vacuum and a family of superpotentials W_M that are not. The question that we wish to address now is how the superpotentials defined at a maximum of V are related to those defined at an ‘adjacent’ minimum of V . A number of single-scalar supergravity models have a potential with a single adS maximum and a single adS minimum, derived from a superpotential with respect to which the maximum is supersymmetric and the minimum is not. The expansion of this superpotential about the minimum necessarily coincides with W_M for some value of M , and it appears from inspection of a few cases that it should be identified with W_- at the maximum. In any case, any supergravity model automatically gives us at least one superpotential that is defined as a single-valued function for all values of the scalar field and hence for all values in the interval between the maximum and the minimum. Let us assume that we are given one such superpotential, not necessarily arising from a supergravity model, and ask about the other potentials. There are evidently various possibilities. It could be that each superpotential that is perturbatively defined at the maximum of V continues to one that is perturbatively defined at the minimum. Alternatively, it could be that a pair of superpotentials defined perturbatively at, say, the maximum are actually two branches of a double-valued potential that is not defined at the minimum. It follows from recent work of Amsel et al. [15] that there exist potentials for which this latter possibility is realized. We now present a version of their argument adapted to our needs.

We assume (i) that $V(\sigma)$ has an adS maximum, at $\sigma = 0$, and an adS minimum at $\sigma = \sigma_+$ but no other stationary points, (ii) that the continuation of W_+ , perturbatively defined at the origin, leads to a function that is single valued in the interval $[0, \sigma_+]$, (ii) that this function is stationary at $\sigma = \sigma_+$. What can we say under these circumstances about the continuation of the function W_- defined at the origin? Both

⁷This generalizes an observation in [1] for the $m^2 = 0$ case of constant V : in that case $W_- = W_0$ and $W_+ = W_0 \cosh(\alpha\sigma)$ for constant W_0 but whereas both W_+ and W_- admit supersymmetric adS vacua only W_+ admits a supersymmetric domain wall.

ν_+ and ν_- are real and positive at the origin, by hypothesis, so not only are both W_+ and W_- positive near $\sigma = 0$ but so also are their derivatives W'_+ and W'_- , as one sees from (4.17). Writing (4.1) as

$$\sqrt{2} W' = \sqrt{V + 2\alpha^2 W^2}, \quad (4.19)$$

we see that it remains true that $W_+ > W_-$ as we increase σ from zero, until a zero of either W_+ or W_- is reached. Since the function $V + 2\alpha^2 W_+^2$ is strictly greater than the function $V + 2\alpha^2 W_-^2$, and since the former is zero at $\sigma = \sigma_+$, there is necessarily a zero of W'_- at some $\sigma_- < \sigma_+$. A priori, this might be another stationary point of V (which would have to be some solution of $W''_+ = \alpha^2 W_+$ since it is not a solution of $W'_+ = 0$, by hypothesis) but this is excluded by assumption (i), so W_- is stationary at a point that is not a stationary point of V . as we have seen, this implies that W_- is a double-valued function that is not defined for $\sigma > \sigma_-$. The simplest possibility for the second branch of this function is that it continues back to the origin, where it must be identified with W_M for some M .

There is a simple interpretation of this result for the cosmological analog in which the potential is inverted. What was a domain wall becomes a cosmology, represented by the damped motion of a ball in the inverted potential $-V$. The adS maximum at the origin becomes a de-Sitter (dS) minimum and the adS minimum at $\sigma = \sigma_+$ a dS maximum. The condition that the BF bound is satisfied at the adS maximum becomes the condition that motion at the dS minimum is overdamped [14], so that it approaches monotonically and exponentially fast with exponent ν_+ or ν_- . Suppose that the ball is initially at rest at the maximum and (after an infinite time) it falls to the minimum, exponentially fast with exponent ν_+ . This cosmological motion corresponds to a domain wall interpolating between the two stationary points of the potential, and it determines a superpotential that (a) is single-valued in the interval $[0, \sigma_+]$, (b) coincides with W_+ at the origin, and (c) is stationary at $\sigma = \sigma_+$. This is the superpotential W_+ of the previous paragraph. We have assumed its existence but this must require a special choice of V since the ball would typically overshoot, yielding a superpotential with a supersymmetric adS maximum and non-supersymmetric adS minimum.

Now suppose that we choose initial conditions for a ball on the other side of the dS minimum such that it overshoots the dS minimum at the origin with non-zero velocity and continues up the potential towards the maximum. It cannot ‘just reach’ the maximum (because that motion has already been accounted for) so it will either overshoot or it will fall back. There must be some initial conditions for which the latter possibility is realized. As it falls back it will either overshoot again or it will approach the dS minimum exponentially fast with exponent ν_- . Although the former possibility may be generic, there must exist some choice of initial conditions that realizes the latter. In this case the corresponding domain wall solution determines the double-valued potential for which the function W_- defined at the origin is one branch, the other branch being a W_M function for some particular M (which carries the information about the required initial conditions in the mechanical interpretation). The branch point of this double-valued function is the turning point in the motion of the ball as it falls back towards the minimum.

4.2 E Pluribus Unum?

We now turn to multi-scalar models. For a generic multi-scalar model, both the potential and the Killing spinor equation must depend on both the superpotential and the target space metric, both of which will generically depend on all scalar fields, because this feature is already apparent from the two-scalar models obtained by coupling of a chiral supermultiplet to $d = 4$ supergravity. Moreover, there will be additional requirements for supersymmetry arising from the requirement of vanishing supersymmetry variations for the spinor superpartners of the additional fields. However, a domain-wall solution of a multi-scalar model can always be viewed as a solution of a single-scalar model obtained by truncation after choosing ‘adapted’ coordinates on the scalar field target space for which all scalar fields but one are constant [16]. As the additional conditions required for supersymmetry are just the constancy of the ‘other’ scalar fields, the problem of (fake) supersymmetry for multi-scalar model domain-walls has been reduced to the single-scalar problem.

However, there is a difficulty with this ‘reduced’ notion of fake supersymmetry (in addition to possible global problems arising from the local nature of the ‘adapted’ target space coordinates). It may happen, if the single-scalar truncation is inconsistent, that there are no nearby solutions of the single-scalar model that are also solutions of the multi-scalar model, in which case the fake supersymmetry of the domain wall as a solution of the single-scalar model is irrelevant to its stability as a solution of the multi-scalar model. We shall show that precisely this scenario is realized by the exact solution of subsection 3.3.

The relation (3.29) satisfied by the axion-domain wall solution of subsection 3.3 suggests that we choose adapted coordinates $(\tilde{\sigma}, \tilde{\chi})$ defined by

$$e^{\mu\sigma} = \exp\left(\frac{\mu}{\sqrt{J_0}}\tilde{\sigma}\right) J \quad \chi - \chi_0 = \exp\left(-\frac{\mu}{2\sqrt{J_0}}\tilde{\sigma}\right) (\tilde{\chi} + \kappa) J^{-1/2}, \quad (4.20)$$

where κ is the constant defined in (3.27), and

$$J = 1 + \frac{1}{4}\mu^2(\tilde{\chi} + \kappa)^2, \quad J_0 = 1 + \frac{1}{4}\mu^2\kappa^2 \equiv \frac{\lambda(\lambda - \mu)}{\lambda_h^2}. \quad (4.21)$$

Observe that $J_0 \geq 1$ for $\mu \leq \mu_c$, and that the Jacobian of this change of variables is non-zero for all finite σ , so the adapted coordinates are valid globally as long as there are no identifications on the hyperbolic target space (e.g. those arising from requiring periodicity in χ). In the new coordinates the solution is

$$\tilde{\chi} = 0, \quad \tilde{\sigma} = \sqrt{J_0} \left[\sigma(z) - \frac{1}{\mu} \ln J_0 \right], \quad \varphi = \varphi(z), \quad (4.22)$$

with $\sigma(z)$ and $\varphi(z)$ as in (3.28). This confirms that the new coordinates are indeed ‘adapted’ to the solution in the sense of [16].

In the gauge used to find the above solution, the effective Lagrangian in the new variables is

$$2L_{eff} = e^{\alpha\varphi - \frac{1}{2}\tilde{\lambda}\tilde{\sigma}} J^{-\frac{\lambda}{2\mu}} (\dot{\varphi}^2 - (J/J_0)\dot{\tilde{\sigma}}^2 - J^{-1}\dot{\tilde{\chi}}^2 - 2\Lambda) \quad (4.23)$$

where

$$\tilde{\lambda} = \lambda / \sqrt{J_0} \equiv \lambda_h \sqrt{\frac{\lambda}{\lambda - \mu}}, \quad (4.24)$$

and the constraint is

$$\dot{\varphi}^2 - (J/J_0) \dot{\tilde{\sigma}}^2 - J^{-1} \dot{\tilde{\chi}}^2 + 2\Lambda = 0. \quad (4.25)$$

Now observe that

$$\tilde{L}_{eff} \equiv (J_0)^{\frac{\lambda}{2\mu}} L_{eff} \Big|_{\tilde{\chi} \equiv 0} = \frac{1}{2} \tilde{f}^{-1} (\dot{\varphi}^2 - \dot{\tilde{\sigma}}^2) - \tilde{f} \Lambda e^{-\tilde{\lambda} \tilde{\sigma}}, \quad (4.26)$$

where

$$\tilde{f} = e^{-\alpha\varphi + \frac{1}{2}\tilde{\lambda}\tilde{\sigma}}, \quad (4.27)$$

and that the equation of motion for \tilde{f} , for \tilde{f} as given, is

$$\dot{\varphi}^2 - \dot{\tilde{\sigma}}^2 + 2\Lambda = 0, \quad (4.28)$$

which is the constraint (4.25) for $\tilde{\chi} \equiv 0$. We see that the ‘adapted’ truncation, achieved by setting $\tilde{\chi} \equiv 0$, yields a one scalar model with exponential potential.

The above construction guarantees that the solution used in the construction of the ‘adapted’ single-scalar model is a solution of the equations of motion of this model. Let us verify this: the solution for $(\varphi, \tilde{\sigma})$, expressed in terms of $\tilde{\lambda}$, is such that⁸

$$\dot{\varphi} = \pm \lambda_h \sqrt{\frac{2\Lambda}{\tilde{\lambda}^2 - \lambda_h^2}}, \quad \dot{\tilde{\sigma}} = \pm \tilde{\lambda} \sqrt{\frac{2\Lambda}{\tilde{\lambda}^2 - \lambda_h^2}}. \quad (4.29)$$

This is precisely the “type 1” fixed point solution of the single-scalar model described in [1], which was shown in that reference to correspond to a flat domain wall solution that is supersymmetric with respect to the real superpotential

$$\tilde{W}(\tilde{\sigma}) = \left(\frac{2\Lambda}{\tilde{\lambda}^2 - \lambda_h^2} \right)^{\frac{1}{2}} \exp \left(-\frac{1}{2} \tilde{\lambda} \tilde{\sigma} \right). \quad (4.30)$$

It follows that there is at least one solution of the single-scalar model that is also a solution of the original axion-dilaton model: namely, the solution of the latter used to construct the former. However, it is not guaranteed that any other solution of the single-scalar model will share this property; it will if the truncation is consistent, in the technical sense, but not necessarily if the truncation is not consistent. For the case in hand, the truncation is *not* consistent: the expansion of L_{eff} in powers of $\tilde{\chi}$ shows that there is a linear term, which is such that the field equation for $\tilde{\chi}$ is satisfied by $\tilde{\chi} \equiv 0$ iff

$$\kappa (\dot{\tilde{\sigma}}^2 - 2\Lambda \lambda / \mu) = 0. \quad (4.31)$$

⁸From (4.24) it follows that $\lambda \neq \lambda_h$ as long as $\mu \neq 0$, as assumed.

This is satisfied if $\kappa = 0$, but this corresponds to the limiting case in which $\dot{\chi} = 0$, so the truncation is equivalent to setting the axion field to zero in the original Lagrangian; this is evidently a consistent truncation, and we implicitly used this fact in section 2. Otherwise, the truncation is inconsistent because it implies a condition on $\tilde{\sigma}$. Using the relation between $\tilde{\sigma}$ and σ at $\tilde{\chi} = 0$, and the constraint, we see that this condition states that

$$\dot{\sigma}^2 = \lambda_h^2 A^2, \quad \dot{\varphi}^2 = (\lambda - \mu)^2 A^2, \quad (4.32)$$

where A is the constant defined in (3.27). As one sees from (3.28), this is satisfied by the solution we started with (as was guaranteed) but *only* by this solution⁹.

4.3 Axion-dilaton fake supergravity

The above result suggests that we should extend the notion of fake supersymmetry to models involving at least an axion as well as a dilaton. Here we consider such an extension, using the coupling of $d = 4$ supergravity to a complex chiral superfield as a model. Consider a Lagrangian density of the form

$$\mathcal{L} = \sqrt{-\det g} [R - 2G \partial\tau \cdot \partial\bar{\tau} - V], \quad (4.33)$$

where τ is a complex scalar field taking values in a Kähler target space and

$$G = \partial_\tau \partial_{\bar{\tau}} \mathcal{K}(\tau, \bar{\tau}) \quad (4.34)$$

is the Kähler target space metric, expressed in terms of the Kähler potential \mathcal{K} . We take the scalar field potential $V(\tau, \bar{\tau})$ to be given in terms of K and a holomorphic superpotential $P(\tau)$ according to the formula

$$V = \frac{1}{2} e^K [|\partial_\tau P + \partial_\tau \mathcal{K} P|^2 G^{-1} - 4\alpha^2 |P|^2]. \quad (4.35)$$

This generalizes to arbitrary d the standard $d = 4$ formula¹⁰. For arbitrary even dimension d , we may similarly generalize the $d = 4$ Killing spinor equation to

$$\left[D_\mu - \frac{1}{2(d-2)} e^{K/2} [\text{Re } P + i\gamma_* \text{Im } P] \Gamma_\mu \right] \epsilon = 0, \quad (4.36)$$

where γ_* is the product of the d Dirac matrices¹¹.

To show that the d -dependence of the coefficients is correct, we write

$$\tau = \chi + i\Phi(\sigma), \quad (4.37)$$

⁹The consistency constraint allows for the sign of $\dot{\sigma}/\dot{\varphi}$ to differ from (3.28) but there is no solution corresponding to this possibility.

¹⁰See, e.g., [20], but note that this reference uses conventions that differ from ours.

¹¹It is possible that it will ultimately be necessary to further restrict d to arrange for $\gamma_*^2 = 1$, as in $d = 4$, but we will not need to pursue this here, for a reason that will shortly be clear.

for some function Φ of the dilaton field σ , and we assume that \mathcal{K} can be written as

$$\mathcal{K} = 2 \log W, \quad (4.38)$$

for some real function W of σ *alone*. In order to get the standard kinetic term for σ , we must choose the functions $W(\sigma)$ and $\Phi(\sigma)$ to be related by the equation

$$\left(\frac{W'}{W}\right)' - \left(\frac{\Phi''}{\Phi'}\right) \left(\frac{W'}{W}\right) = \frac{1}{2}, \quad (4.39)$$

where a prime indicates a derivative with respect to σ . Specifically, this equation implies that

$$2G \partial\tau \cdot \partial\bar{\tau} = \frac{1}{2} \left[(\partial\sigma)^2 + (\Phi')^{-2} (\partial\chi)^2 \right]. \quad (4.40)$$

If we now consider $P = 1$, then we find that the formula (4.35) reduces to the standard d -dimensional fake-supergravity formula

$$V = 2 \left[(W')^2 - \alpha^2 W^2 \right], \quad (4.41)$$

and the equation (4.36) reduces to the standard d -dimensional fake Killing spinor equation¹² (4.2). As the potential (4.41) is independent of χ , it is clearly consistent to set χ to a constant, and in this case we recover the standard single-scalar fake supersymmetry set-up in the conventions of [1]. We will not do this here since the solution of interest is one for which χ is not constant. Furthermore, the truncation in adapted variables that *is* compatible with the solution of interest is not compatible with any other solution, as we have seen, so *there is no truncation that is both consistent and compatible with the solution of interest*. We therefore proceed *without* truncation, in which case it is important to appreciate that both the expression for the potential (4.41) and the Killing spinor equation (4.2) are valid generally, as long as $P = 1$. Although we considered the choice $P = 1$ for the purpose of verifying the correctness of the d -dependence of the coefficients in the expressions (4.41) and (4.36), this choice (which one may make without loss of generality as soon as it is assumed that P is a non-zero constant) is also the only obvious one that leads to a potential depending *only* on the dilaton, and there seems to be no other choice that leads to the specific axion-independent exponential potential of our family of axion-dilaton models¹³. For this reason, the choice $P = 1$ will continue to play a role in what follows. Note that for $P = 1$ the restriction that we made to even d can be relaxed, since (4.2) makes sense for any d .

Observe now that the kinetic term for the axion in (4.40) involves the function $\Phi(\sigma)$. Our axion-dilaton model is found by choosing

$$\Phi = \pm \frac{2}{\mu} e^{-\frac{\mu}{2}\sigma}, \quad (4.42)$$

¹²These formulae are exactly those used in [1], as they should be since our conventions are the same.

¹³The choice $P \propto \tau$ also leads to an axion-independent potential for an appropriate choice of W , but this yields neither the target space metric nor the scalar potential of our models.

in which case (4.39) reduces to

$$\left(\frac{W'}{W}\right)' + \frac{\mu}{2} \left(\frac{W'}{W}\right) = \frac{1}{2}, \quad (4.43)$$

This equation is solved by¹⁴

$$W = W_0 e^{\sigma/\mu}, \quad (4.44)$$

for constant W_0 . If we also assume that $P = 1$, so that (4.41) applies, then we have the potential

$$V = \Lambda e^{-\lambda\sigma} \quad (4.45)$$

where

$$\lambda = -2/\mu, \quad 2\Lambda = W_0^2 (\lambda^2 - \lambda_h^2). \quad (4.46)$$

What we have now shown is that a one-parameter subfamily of our two-parameter family of axion-dilaton models may be considered as ‘fake axion-dilaton supergravities’, in the sense described above. This family is defined by $\mu\lambda = -2$ and includes the Einstein-dilaton truncation of the $d = 4$ FS model as a special case.

Actually, we have two separate one-parameter families: one with $\Lambda > 0$ and $\lambda > \lambda_h$ and another with $\Lambda < 0$ and $\lambda < \lambda_h$. In either case we have $\mu(\lambda - \mu) < 0$ (since $\mu = -2/\lambda < 0$) and hence the restriction to the one-parameter family is compatible with the existence of the fixed point solution discussed above only if $\Lambda < 0$, and it exists in this case only if $\mu \leq \mu_c$. In the special case that $\mu = \mu_c$, which is realized by the FS model, we see from (3.29) that $\dot{\chi} = 0$, and hence that the $\chi = 0$ truncation $\chi = 0$ is consistent. We shall exclude this case as trivial (the solution coincides with one of the fixed-point solutions of section 2) so we consider only $\mu < \mu_c$, which is equivalent to $\lambda > \lambda_c$ when $\mu\lambda = -2$. To summarise, a fixed point solution with non-constant χ exists for $\mu = -2\lambda$ and $\Lambda < 0$ provided that

$$\lambda_c < \lambda < \lambda_h. \quad (4.47)$$

Observe that

$$W = K e^{-\frac{1}{2}\lambda\sigma}, \quad K = \sqrt{\frac{2\Lambda}{\lambda^2 - \lambda_h^2}} \quad (4.48)$$

for this 1-parameter family, and that W and \tilde{W} , of (4.30), are identical functions of their arguments, as expected since the ‘adapted’ truncation leading to the superpotential $\tilde{W}(\tilde{\sigma})$ coincides with the consistent truncation $\dot{\chi} \equiv 0$ leading to the superpotential $W(\sigma)$ in the limit that $\lambda = \lambda_c$.

These fixed point solutions are fake supersymmetric in the sense of [5], which relies on the truncation in ‘adapted’ coordinates of [16], but are they fake supersymmetric solutions of the untruncated model? We are now in a position to answer this question. First, we recall from [1] that the integrability conditions for the Killing spinor equation (4.2) are

$$\dot{\varphi} = \pm 2\alpha e^{\frac{1}{2}\lambda\sigma} W, \quad \dot{\sigma} = \mp 2e^{\frac{1}{2}\lambda\sigma} W', \quad (4.49)$$

¹⁴Other solutions of (4.43) yield a ‘non-exponential’ potential that is of no particular interest here.

and hence, for the superpotential (4.44),

$$\dot{\varphi} = \pm 2\alpha W_0, \quad \dot{\sigma} = \pm \lambda W_0. \quad (4.50)$$

Comparing with (3.28) we see that supersymmetry requires $W_0 = \sqrt{|\Lambda|}$ and $\mu = \mu_c$ or, equivalently, $\lambda = \lambda_c$, which is outside the range (4.47). The fake supersymmetry of the limiting case for which $\lambda = \lambda_c$ is not surprising because $\dot{\chi} = 0$ in this case. In all cases for which the axion is not constant, the single-scalar truncation is inconsistent, the domain-wall solution is *not* a fake supersymmetric solution of the untruncated model, at least not in the sense described here.

5 Discussion

We have studied domain wall solutions of gravity coupled to an axion and dilaton, with a hyperbolic target space and exponential dilaton potential. In particular, we have studied the dependence on the two parameters $\mu \neq 0$ and $\lambda \geq 0$ that determine, respectively, the target space radius and the dilaton self-coupling. Starting from the observation that domain wall solutions with either (i) constant dilaton or (ii) Minkowski ‘worldvolume’ are essentially determined by the trajectories of an autonomous 2-dimensional dynamical system, we have used the methods of dynamical systems to provide an analysis of the trajectories in these two cases, allowing for either sign of the potential. In case (i) our results constitute a global completion of previous results. In case (ii) we have both extended previous results to either sign potential, and provided a global completion of them. In both cases this has been achieved by finding appropriate new variables that allow the global picture to emerge naturally. We have also investigated the nature of the bifurcations that occur when fixed points coincide as the parameters vary. All simple bifurcations are transcritical. We should stress here that these dynamical systems results are equally applicable to domain-walls and cosmologies, but we have focused here on the domain-wall interpretation to avoid any confusion that may arise from the flip of the sign of the potential, and curvature k , needed to pass from one interpretation to the other.

One new result of this paper is an exact solution for a flat domain wall with non-constant axion field. For one sign of the potential (negative for domain walls but positive for cosmology) this is the domain wall solution that corresponds to the cosmological scaling solution found in [8]. In this context, it was noted by Rosseel et al. [21] that this solution is unusual in that the motion in the target space is not geodesic, and the same observation obviously applies in the domain wall case. We have used this solution as a ‘laboratory’ for a detailed investigation of the notion of ‘fake’ supergravity in models with more than one scalar field.

As shown in [4, 1, 5], *all* flat or adS-sliced domain wall solutions for which the scalar field is a strictly monotonic function are supersymmetric with respect to a superpotential that is determined by the solution itself. The monotonicity condition is violated ‘maximally’ by adS vacua and ‘badly’ by domain walls that are asymptotic to unstable adS vacua. Here we have investigated what happens when it is violated at isolated points, which is a fairly generic phenomenon. An explicit example confirmed

the suggestion of [5] that such domain walls should be ‘piecewise supersymmetric’ with respect to a multi-valued superpotential. It also showed how this is associated with stationary points of the superpotential that are not stationary points of the potential. A nice picture emerged from our further investigation of multi-valued superpotentials in which the domain wall solutions of any given potential determine the global branched structure of the associated superpotential, or superpotentials, and we used this to recover and extend results of [15] on negative potentials with both a fake supersymmetric maximum and a fake supersymmetric minimum.

There is a sense in which the results on supersymmetry of domain walls in single-scalar models carry over, at least locally, to multi-scalar models because any domain-wall solution of a multi-scalar model is also a solution of the single-scalar model obtained by truncation in ‘adapted’ target-space coordinates [16]. Obviously, one cannot expect to use fake supersymmetry in this sense to prove stability with respect to fluctuations of the truncated scalars but one might hope that it would be sufficient for stability against fluctuations of the one untruncated scalar. The results of this paper show that this hope is unfounded, in general. The problem is that the ‘adapted’ truncation is not guaranteed to be a consistent one, and if it is not consistent then the ‘nearby’ (and generically, time-dependent) solutions of the single-scalar model (needed to establish stability in the single-scalar context) do not lift to ‘nearby’ solutions of the original multi-scalar model. We have shown that the new exact solutions mentioned above has precisely this feature, which we suspect is related to the non-geodesic property noted in [21].

One might still hope to establish stability of at least a large class of axion-dilaton domain walls by a more direct extension of the methods of fake supergravity to multi-scalar models. We have made a start on this program, using the coupling of $d = 4$ supergravity to a chiral supermultiplet as a model. We have shown how the usual single-scalar fake supergravity formulae can be viewed as special cases of more general scalar-pseudoscalar fake supergravity formulae, but our axion-dilaton models become fake supergravities within this framework only for a one-parameter subfamily of the two-parameter family investigated here, although it remains possible that this restriction could be lifted by a more general notion of axion-dilaton fake supergravity that does not assume a Kähler target space. Fortunately, the one-parameter restriction is compatible with the existence of our new exact solution for $\Lambda < 0$, and we were able to show that this solution is *not* fake supersymmetric in our extended sense, even though it *is* a fake supersymmetric solution of the single-scalar model obtained by adapted truncation. We believe that this a consequence of the inconsistency of this truncation.

Acknowledgements

We thank Alessio Celi, Jonathan Dawes, Joaquim Gomis, Kostas Skenderis and Antoine Van Proeyen for helpful conversations.

References

- [1] J. Sonner and P. K. Townsend, *Dilaton domain walls and dynamical systems*, Class. Quant. Grav. **23**, 441 (2006) [arXiv:hep-th/0510115].
- [2] J. J. Halliwell, *Scalar Fields In Cosmology With An Exponential Potential*, Phys. Lett. B **185** (1987) 341.
- [3] A. B. Burd and J. D. Barrow, *Inflationary models with exponential potentials*, Nucl. Phys. B **308** (1988) 929.
- [4] D. Z. Freedman, C. Nuñez, M. Schnabl and K. Skenderis, *Fake supergravity and domain wall stability*, Phys. Rev. D **69**, 104027 (2004) [arXiv:hep-th/0312055].
- [5] K. Skenderis and P. K. Townsend, *Hidden supersymmetry of domain walls and cosmologies*, Phys. Rev. Lett. **96** (2006) 191301 [arXiv:hep-th/0602260]; *Pseudo-supersymmetry and the domain-wall/cosmology correspondence*, in proceedings of IRGAC 2006 [arXiv:hep-th/0610253].
- [6] E. Bergshoeff, A. Collinucci, U. Gran, M. Nielsen and D. Roest, *Transient quintessence from group manifold reductions or how all roads lead to Rome*, Class. Quant. Grav. **21** (2004) 1947 [arXiv:hep-th/0312102].
- [7] P. K. Townsend and M. N. R. Wohlfarth, *Cosmology as geodesic motion*, Class. Quant. Grav. **21** (2004) 5375 [arXiv:hep-th/0404241].
- [8] J. Sonner and P. K. Townsend, *Recurrent acceleration in dilaton-axion cosmology*, Phys. Rev. D **74** (2006) 103508 [arXiv:hep-th/0608068].
- [9] A. P. Billyard, A. A. Coley and J. E. Lidsey, *Cyclical behaviour in early universe cosmologies*, J. Math. Phys. **41** (2000) 6277 [arXiv:gr-qc/0005118].
- [10] D. Z. Freedman and J. H. Schwarz, *$N=4$ Supergravity Theory With Local $SU(2) \times SU(2)$ Invariance*, Nucl. Phys. B **137** (1978) 333.
- [11] P. K. Townsend, *Positive Energy And The Scalar Potential In Higher Dimensional (Super)Gravity Theories*, Phys. Lett. B **148** (1984) 55.
- [12] K. Skenderis and P. K. Townsend, *Gravitational stability and renormalization-group flow*, Phys. Lett. B **468** (1999) 46 [arXiv:hep-th/9909070].
- [13] O. DeWolfe, D. Z. Freedman, S. S. Gubser and A. Karch, *Modeling the fifth dimension with scalars and gravity*, Phys. Rev. D **62** (2000) 046008 [arXiv:hep-th/9909134].
- [14] K. Skenderis and P. K. Townsend, *Hamilton-Jacobi method for domain walls and cosmologies*, Phys. Rev. D **74** (2006) 125008 [arXiv:hep-th/0609056].
- [15] A. J. Amsel, T. Hertog, S. Hollands and D. Marolf, *A tale of two superpotentials: Stability and instability in designer gravity*, arXiv:hep-th/0701038.

- [16] A. Celi, A. Ceresole, G. Dall'Agata, A. Van Proeyen and M. Zagermann, *On the fakeness of fake supergravity*, Phys. Rev. D **71** (2005) 045009 [arXiv:hep-th/0410126].
- [17] P. M. Cowdall, *Supersymmetric electrovac in gauged supergravities*, Class. Quant. Grav. **15** (1998) 2937 [arXiv:hep-th/9710214].
- [18] P. Breitenlohner and D. Z. Freedman, *Positive Energy In Anti-De Sitter Backgrounds And Gauged Extended Supergravity*, Phys. Lett. B **115** (1982) 197; *Stability In Gauged Extended Supergravity*, Annals Phys. **144** (1982) 249.
- [19] L. Mezincescu and P. K. Townsend, *Stability At A Local Maximum In Higher Dimensional Anti-De Sitter Space And Applications To Supergravity*, Annals Phys. **160**, 406 (1985).
- [20] J. Bagger, *Supersymmetric Sigma Models*, SLAC-PUB-3461 *Lectures given at Bonn-NATO Advanced Study Inst. on Supersymmetry, Bonn, West Germany, Aug 20-31, 1984*
- [21] J. Rosseel, T. Van Riet and D. B. Westra, *Scaling cosmologies of $N = 8$ gauged supergravity*, arXiv:hep-th/0610143.